

AD693987

NOLTR 69-52

A TIME-DEPENDENT ANALYSIS FOR QUASI-  
ONE-DIMENSIONAL NOZZLE FLOWS WITH  
VIBRATIONAL AND CHEMICAL  
NONEQUILIBRIUM

By  
John D. Anderson, Jr.

NOL

MAY 1969

D D C  
OCT 6 1969

UNITED STATES NAVAL ORDNANCE LABORATORY, WHITE OAK, MARYLAND

NOLTR 69-52

ATTENTION

This document has been approved for  
public release and sale, its distribution  
is unlimited.

NOLTR 69-52

A TIME-DEPENDENT ANALYSIS FOR  
QUASI-ONE-DIMENSIONAL NOZZLE FLOWS WITH  
VIBRATIONAL AND CHEMICAL NONEQUILIBRIUM

Presented by:  
John D. Anderson, Jr.

**ABSTRACT:** A new technique is presented for the numerical solution of quasi-one-dimensional, vibrational and chemical nonequilibrium nozzle flows including nonequilibrium conditions both upstream and downstream of the throat. This new technique is a time-dependent analysis which entails the explicit finite-difference solution of the quasi-one-dimensional unsteady flow equations in steps of time, starting with assumed initial distributions throughout the nozzle. The steady-state solution is approached at large values of time. A virtue of the present time-dependent analysis is its simplicity, which prevails from its initial physical formulation to the successful receipt of numerical results. Also, the present solution yields the transient as well as the steady-state nonequilibrium nozzle flows. To exemplify the present analysis, results are given for several cases of vibrational and chemical nonequilibrium expansions through nozzles.

U. S. NAVAL ORDNANCE LABORATORY  
White Oak, Maryland

NOLTR 69-52

A Time-Dependent Analysis for Quasi-One-Dimensional Nozzle Flows  
With Vibrational and Chemical Nonequilibrium

This report presents a new technique for the numerical solution of quasi-one-dimensional nonequilibrium nozzle flows. The governing equations and numerical approach are discussed in detail, and results are presented for the cases of a calorically perfect gas, vibrational nonequilibrium and chemical nonequilibrium.

This work was performed jointly under the support of the Independent Research (IR) Program of the Naval Ordnance Laboratory, Problem 088, and the Fluid Mechanics Branch of the Office of Naval Research.

E. F. SCHREITER  
Captain, USN  
Commander

*L. H. Schindel*  
L. H. SCHINDEL  
By direction

NOLTR 69-52

CONTENTS

	Page
INTRODUCTION.....	1
ANALYSIS.....	3
Calorically Perfect Gas.....	7
Vibrational Nonequilibrium.....	8
Chemical Nonequilibrium.....	11
Comments on the Numerical Solution.....	17
RESULTS.....	20
Calorically Perfect Gas.....	21
Vibrational Nonequilibrium.....	22
Influence of Subsonic Area Distribution.....	24
Chemical Nonequilibrium.....	25
CONCLUSIONS.....	27

ILLUSTRATIONS

Figure

- 1 Sketch of the Coordinate System and Grid Points
- 2 Transient and Final Steady-State Temperature Distributions for a Calorically Perfect Gas Obtained from the Present Time-Dependent Analysis;  $\gamma = 1.4$
- 3 Transient and Final Steady-State Mass-Flow Distributions for a Calorically Perfect Gas Obtained from the Present Time-Dependent Analysis;  $\gamma = 1.4$
- 4 Steady-State Pressure and Velocity Distributions for a Calorically Perfect Gas; Comparison of the Present Time-Dependent Analysis with Results Obtained from Reference 18
- 5 Transient and Final Steady-State  $e_{vib}$  Distributions for the Nonequilibrium Expansion of  $N_2$  Obtained from the Present Time-Dependent Analysis
- 6 Steady-State  $T_{vib}$  Distributions for the Nonequilibrium Expansion of  $N_2$ ; Comparison of the Present Time-Dependent Analysis with the Steady-Flow Analysis of Reference 13
- 7 Steady-State  $T_{vib}$  and  $T_{trans}$  Distributions for the Nonequilibrium Expansion of  $N_2$ ; Comparison of the Present Time-Dependent Analysis with the Steady-Flow Analysis of Reference 7
- 8 Steady-State Pressure and Velocity Distributions for the Nonequilibrium Expansion of  $N_2$ ; Comparison of the Present Time-Dependent Analysis with the Steady-Flow Analysis of Reference 7
- 9 Steady-State  $e_{vib}$  Distributions for the Nonequilibrium Expansion of  $N_2$ ; Comparison of the Present Time-Dependent Analysis with the Steady-Flow Analysis of Reference 8
- 10 Comparison of  $T_{vib}$  Distributions for Two Nozzles with Different Subsonic Sections but Identical Supersonic Sections;  $p_0 = 80$  atm, Nonequilibrium Expansion of  $N_2$
- 11 Comparison of  $T_{vib}$  Distributions for Two Nozzles with Different Subsonic Sections but Identical Supersonic Sections;  $p_0 = 10$  atm, Nonequilibrium Expansion of  $N_2$
- 12 Transient and Final Steady-State Atom Mass-Fraction Distributions for the Nonequilibrium Expansion of Dissociating Oxygen Obtained from the Present Time-Dependent Method; the Steady-State Distribution is Compared with the Steady-Flow Analysis of Reference 2

Figure

- 13      Variation of Atomic Mass Fraction at the Nozzle Exit  
         as a Function of Time
- 14      Steady-State Atom Mass-Fraction Distribution for the  
         Nonequilibrium Expansion of Dissociating Oxygen;  
         Comparison of the Present Time-Dependent Analysis  
         with the Steady-Flow Analysis of Reference 2
- 15      Steady-State Temperature Distribution for the Non-  
         equilibrium Expansion of Dissociating Oxygen;  
         Comparison of the Present Time-Dependent Analysis  
         with the Steady-Flow Analysis of Reference 2
- 16      Steady-State Density Distribution for the Nonequi-  
         librium Expansion of Dissociating Oxygen; Comparison  
         of the Present Time-Dependent Analysis with the Steady-  
         Flow Analysis of Reference 2
- 17      Steady-State Pressure Distribution for the Nonequi-  
         librium Expansion of Dissociating Oxygen; Comparison  
         of the Present Time-Dependent Analysis with the Steady-  
         Flow Analysis of Reference 2

NOMENCLATURE

- $A$  = cross-sectional area, also symbol for atomic species  
 $A'$  =  $A/A^*$   
 $A^*$  = area of throat  
 $a_o$  = reservoir frozen speed of sound  
 $a$  = frozen speed of sound, also a constant in expression for  $\tau$   
 $a'$  =  $a/a_o$   
 $c_v$  = specific heat per unit mass of mixture  
 $C_{v_i}$  = specific heat per mole of species  $i$   
 $D$  = dissociation energy per molecule  
 $E_i$  = internal energy per mole of species  $i$ , including the heat of formation  
 $E_i'$  =  $E_i/E_o$   
 $E_o$  = internal energy of the reservoir mixture  
 $e_{vib}$  = vibrational internal energy per unit mass  
 $e'_{vib}$  =  $e_{vib}/RT_o$   
 $h$  = Planck's constant  
 $k$  = Boltzmann constant  
 $k_F^j$  = forward reaction rate constant  
 $k_R^j$  = reverse reaction rate constant;  $k_F^j/k_R^j = K_e$   
 $K_e$  = equilibrium constant  
 $L$  = characteristic length taken equal to length of nozzle  
 $\bar{m}$  = molecular weight of mixture  
 $p$  = pressure  
 $q$  = general nonequilibrium variable in equation (5)  
 $R$  = specific gas constant of the mixture  
 $\mathcal{R}$  = universal gas constant

$t$	= time
$t'$	= $t/(L/a_o)$
$T$	= temperature (translational)
$T'$	= $T/T_o$
$T'_D$	= $D/k$
$u$	= velocity
$u'$	= $u/a_o$
$V$	= $\ln u'$
$\dot{w}_i$	= rate of production of species $i$ due to chemical reactions
$x$	= distance along nozzle
$x'$	= $x/L$
$Z$	= $\ln \rho'$
$\alpha$	= mass fraction of atomic species in a dissociating gas
$\gamma$	= $c_p/c_v$
$\Gamma_i$	= $\ln \eta_i'$
$\eta_i$	= mole-mass ratio of species $i$ (moles of $i$ per unit mass of mixture)
$\eta_i'$	= $\eta_i/\eta_o$
$\eta_o$	= mole-mass ratio of the reservoir mixture
$\theta$	= $\ln(e'_{vib})$
$\rho$	= density
$\rho'$	= $\rho/\rho_o$
$\nu$	= characteristic vibrational frequency
$\tau$	= vibrational relaxation time
$\tau'$	= $\tau/(L/a_o)$
$\phi$	= $\ln T'$



Subscripts

- i = chemical species i
- o = reservoir conditions
- A = atomic species
- $\Lambda_2$  = diatomic species

Superscript

- j = collision partner in equation (14)

# INTRODUCTION

Because of the practical importance of high-temperature flows through rocket nozzles and high-enthalpy aerodynamic testing facilities, intensive efforts have been made during the past decade to obtain relatively exact numerical solutions for the quasi-one-dimensional expansion of a high-temperature gas through a convergent-divergent nozzle when vibrational and/or chemical nonequilibrium conditions prevail within the gas both upstream and downstream of the throat. (See for example, Refs. 1-6, 10-13, 23-25.) All of these nonequilibrium solutions involve steady-state analyses, and are by no means trivial; however, the evolution of such efforts has produced adequate and sophisticated techniques for the analysis of nonequilibrium nozzle flows. An authoratative discussion of these steady-flow techniques can be found in Ref. 1.

The purpose of the present paper is to present a new, alternative approach for the numerical solution of quasi-one-dimensional nonequilibrium nozzle flows. This new technique is a time-dependent analysis which entails the finite-difference solution of the quasi-one-dimensional unsteady equations of change in steps of time. For specified equilibrium reservoir conditions and a fixed-nozzle shape, the physical gas-dynamic properties are obtained in steps of time, starting with assumed distributions throughout the nozzle. The steady-state solution is approached at large values of time.

The present time-dependent analysis considers vibrational and chemical nonequilibrium conditions both upstream and downstream of the nozzle throat; the proper steady-state critical mass flow is automatically approached at large values of time. In addition, no oscillations and instabilities occur in regions of near equilibrium flow, no special procedures are required to start the solutions from equilibrium reservoir conditions, and very large spacings between grid points can be employed throughout the entire nozzle. (Accurate solutions have been obtained for convergent-divergent nozzles with area ratios of 10 using as few as 15 grid points beginning at the reservoir.) Also, the present method readily handles simultaneous rate processes involving very slow and very fast reactions.

The main virtue of the present time-dependent technique is its simplicity. The governing conservation equations are directly solved by a simple, explicit finite-difference scheme. The technique requires no additional mathematical methods to overcome special difficulties that can occur in the analysis of nonequilibrium flows. (See Ref. 1 for a detailed discussion of these difficulties.) Also, the present technique lends itself to particularly simple programming for a digital computer. Consequently, the simplicity of the present technique prevails from its initial physical formulation to the successful receipt of numerical results.

A second virtue is that the present technique yields the transient as well as the steady-state nonequilibrium nozzle flows.

A transient solution is of interest in its own right; for example, the physical times required for the fluid dynamic and chemical variables to approach their steady-state values can be assessed.

### ANALYSIS

The physical problem treated in the present paper is that of the quasi-one-dimensional motion of a high-temperature gas expanding from equilibrium-reservoir conditions through a convergent-divergent nozzle, where the expansion is rapid enough such that vibrational and chemical nonequilibrium prevail locally in both the subsonic and supersonic portions of the flow. (The term "quasi-one-dimensional" will be discussed in a subsequent paragraph.) Vibrational and chemical nonequilibrium are the only dissipation mechanisms assumed in the flow; the effects of thermal conduction, diffusion and viscous dissipation are assumed to be negligibly small. The equilibrium reservoir conditions and nozzle shape are specified, and a solution is sought for the steady-flow distribution of  $\rho$ ,  $u$ ,  $T$ ,  $p$ ,  $e_{vib}$  and chemical composition in the  $x$  direction along the nozzle (see Fig. 1). The unique aspect of the present analysis is that a time-dependent approach is used to obtain the steady-state nonequilibrium nozzle flow variables.

The crux of the present analysis is as follows: For specified equilibrium reservoir conditions and a fixed-nozzle shape, initial values of the flow-field variables  $\rho$ ,  $u$ ,  $T$ ,  $e_{vib}$  and chemical

composition are assumed at equally spaced grid points along the x-axis, as shown in Figure 1. If all flow-field variables are known at time  $t$ , then at each interior grid point new values can be obtained at time  $(t + \Delta t)$  from the first three terms of a Taylor's series expansion in time,

$$g(t + \Delta t) = g(t) + \left(\frac{\partial g}{\partial t}\right)_t \Delta t + \left(\frac{\partial^2 g}{\partial t^2}\right)_t \frac{(\Delta t)^2}{2} \quad (1)$$

where  $g$  signifies  $\ln \rho$ ,  $\ln u$ ,  $\ln T$ ,  $\ln(e_{vib})$ , and  $\ln \eta_i$ , and  $\Delta t$  is a small increment in time chosen to satisfy certain stability criteria discussed in a subsequent section. (For the present numerical computations, the natural logarithms of the nondimensional flow-field variables are employed as the dependent variables in order to improve numerical stability, and a nondimensional time,  $t'$ , is employed in lieu of  $t$  in equation (1).) Starting with the initially assumed gas-dynamic variables at  $t = 0$ , the flow field is subsequently obtained in steps of time from equation (1). At large values of time (after many time steps, usually on the order of 700 or more) the steady-state flow field is obtained, where  $\frac{\partial g}{\partial t}$  and  $\frac{\partial^2 g}{\partial t^2}$  both approach zero. For the present investigation this steady-state solution is the desired result; indeed, the purpose of the present report is to show that the time-dependent approach is simply an advantageous means to the end.

The time derivatives  $\left(\frac{\partial g}{\partial t}\right)_t$  and  $\left(\frac{\partial^2 g}{\partial t^2}\right)_t$  which appear in equation (1) are obtained from the unsteady quasi-one-dimensional conservation equations (the independent variables are  $x$  and  $t$ ). These equations can be derived from the consideration of a fixed

control volume in the flow; they do not necessarily follow from the general three-dimensional partial-differential equations of change (formulated in any good text in gas dynamics, such as Ref. 14) because of the physical inconsistency between the two assumptions of one-dimensional flow and variable cross-sectional area (hence the term "quasi-one-dimensional"). Nevertheless, the quasi-one-dimensional equations are commonly used as a satisfactory approximation for the variation of flow properties through a nozzle; this approximation becomes more accurate as the variation of  $A$  with  $x$  becomes smaller. For a fixed  $A = A(x)$ , the unsteady quasi-one-dimensional equations are:

$$\text{Continuity: } A \frac{\partial \rho}{\partial t} + \frac{\partial (\rho u A)}{\partial x} = 0 \quad (2)$$

$$\text{Momentum: } \rho \frac{\partial u}{\partial t} + \rho u \frac{\partial u}{\partial x} = - \frac{\partial p}{\partial x} \quad (3)$$

$$\text{Energy: } \rho \frac{\partial e}{\partial t} + \rho u \frac{\partial e}{\partial x} = - p \frac{\partial u}{\partial x} - \rho u \frac{\partial (\ln A)}{\partial x} \quad (4)$$

$$\text{Rate: } \frac{\partial q}{\partial t} + u \frac{\partial q}{\partial x} = w(\rho, T, q) \quad (5)$$

$$\text{State: } p = \rho R T \quad (6)$$

where  $q$  denotes a nonequilibrium quantity such as  $e_{\text{vib}}$  or chemical composition, and  $w$  is a function which depends on the type of rate process under consideration. Defining the following nondimensional variables,  $\rho' = \rho/\rho_0$ ,  $u' = u/a_0$ ,  $T' = T/T_0$ ,  $x' = x/L$ ,  $t' = t/(L/a_0)$ ,  $A' = A/A^*$ ,  $Z = \ln \rho'$ ,  $V = \ln u'$ ,  $\phi = \ln T'$ , where the subscript zero denotes reservoir conditions,  $L$  is the length of the nozzle,  $A^*$  is the nozzle throat area, and  $a_0 = (\gamma_0 R_0 T_0)^{1/2}$  is the reservoir

frozen speed of sound, and after replacing p in equation (3) with equation (6), equations (2) and (3) become

$$\frac{\partial Z}{\partial t'} = -u' \left[ \frac{\partial (\ln A')}{\partial x'} + \frac{\partial V}{\partial x'} + \frac{\partial Z}{\partial x'} \right] \quad (7)$$

$$\frac{\partial V}{\partial t'} = - \left( \frac{T'}{\gamma_0 u'} \right) \left( \frac{\partial \phi}{\partial x'} + \frac{\partial Z}{\partial x'} \right) - u' \frac{\partial V}{\partial x'} \quad (8)$$

(Note that equation (8) applies to a nonreacting gas, where  $R =$  constant; for a reacting gas, where  $R$  is variable, equation (8) is slightly modified, as shown in a subsequent section.)

In equations (7) and (8), all  $x$ -derivatives are calculated by central finite differences obtained from the known flow field at time  $t$ . Consequently, equations (7) and (8) directly yield  $\left( \frac{\partial g}{\partial t} \right)_t$  required in equation (1), where  $g = Z$  and  $V$ ;  $\left( \frac{\partial^2 g}{\partial t^2} \right)_t$  can be obtained by differentiating the same equations with respect to time.

$$\frac{\partial^2 Z}{\partial t'^2} = -u' \left[ \frac{\partial^2 V}{\partial x' \partial t'} + \frac{\partial^2 Z}{\partial x' \partial t'} \right] + \left( \frac{\partial V}{\partial t'} \right) \left( \frac{\partial Z}{\partial t'} \right) \quad (7a)$$

$$\begin{aligned} \frac{\partial^2 V}{\partial t'^2} = & - \left( \frac{T'}{\gamma_0 u'} \right) \left[ \frac{\partial^2 \phi}{\partial x' \partial t'} + \frac{\partial^2 Z}{\partial x' \partial t'} + \left( \frac{\partial \phi}{\partial x'} + \frac{\partial Z}{\partial x'} \right) \left( \frac{\partial \phi}{\partial t'} - \frac{\partial V}{\partial t'} \right) \right] \\ & - u' \left( \frac{\partial^2 V}{\partial x' \partial t'} + \frac{\partial V}{\partial x'} \frac{\partial V}{\partial t'} \right) \end{aligned} \quad (8a)$$

However, the above additional time derivatives introduce cross derivatives,  $\frac{\partial^2 g}{\partial x \partial t}$ , which can be obtained by differentiation of equations (7) and (8) with respect to  $x'$ .

$$\frac{\partial^2 Z}{\partial x' \partial t'} = -u' \left[ \frac{\partial^2 (\ln A')}{\partial x'^2} + \frac{\partial^2 V}{\partial x'^2} + \frac{\partial^2 Z}{\partial x'^2} \right] + \left( \frac{\partial V}{\partial x'} \right) \left( \frac{\partial Z}{\partial t'} \right) \quad (7b)$$

$$\begin{aligned}
\frac{\partial^2 V}{\partial x'^2 \partial t'} &= -\left(\frac{T'}{\gamma_0 u'}\right) \left[ \frac{\partial^2 \phi}{\partial x'^2} + \frac{\partial^2 Z}{\partial x'^2} + \left(\frac{\partial \phi}{\partial x'} + \frac{\partial Z}{\partial x'}\right) \left(\frac{\partial \phi}{\partial x'} - \frac{\partial V}{\partial x'}\right) \right] \\
&\quad - u' \left[ \frac{\partial^2 V}{\partial x'^2} + \left(\frac{\partial V}{\partial x'}\right)^2 \right]
\end{aligned} \tag{8b}$$

To complete the formulation of the problem, the nondimensional counterparts of equations (4) and (5) must be obtained. These counterparts have a distinct form for each of the three cases treated in the present paper, namely the cases of a calorically perfect gas, vibrational nonequilibrium, and chemical nonequilibrium. These forms are presented in the following sections.

#### Calorically Perfect Gas

By treating the case of a calorically perfect, nonreacting gas (constant  $\gamma$ ), results have been obtained which illustrate the purely fluid dynamic behavior of the present time-dependent analysis. For a complete formulation of this case, only the energy equation needs to be considered in addition to equations (7) and (8). With  $e = c_v T$  and  $c_v = R/(\gamma - 1)$ , the nondimensional form of equation (4) is

$$\frac{\partial \phi}{\partial t'} = -(\gamma - 1) u' \frac{\partial V}{\partial x'} - u' \frac{\partial \phi}{\partial x'} - (\gamma - 1) u' \frac{\partial \ln A'}{\partial x'} \tag{9}$$

Equation (9) directly yields  $\left(\frac{\partial g}{\partial t}\right)_t$  required in equation (1), where  $g = \phi$ ; as before,  $\frac{\partial^2 g}{\partial t^2}$  and the resulting cross derivative  $\frac{\partial^2 g}{\partial x \partial t}$  are obtained by differentiating equation (9) with respect to  $t'$  and  $x'$  respectively.



$$\begin{aligned} \frac{\partial^2 \phi}{\partial t'^2} = & -(\gamma - 1) u' \left[ \frac{\partial^2 V}{\partial x' \partial t'} + \left( \frac{\partial V}{\partial x'} \right) \left( \frac{\partial V}{\partial t'} \right) + \frac{\partial V}{\partial t'} \frac{\partial (\ln A')}{\partial x'} \right] \\ & - u' \left[ \frac{\partial^2 \phi}{\partial x' \partial t'} + \left( \frac{\partial \phi}{\partial x'} \right) \left( \frac{\partial V}{\partial t'} \right) \right] \end{aligned} \quad (9a)$$

$$\begin{aligned} \frac{\partial^2 \phi}{\partial x' \partial t'} = & -(\gamma - 1) u' \left[ \frac{\partial^2 V}{\partial x'^2} + \left( \frac{\partial V}{\partial x'} \right)^2 + \frac{\partial^2 (\ln A')}{\partial x'^2} + \left( \frac{\partial V}{\partial x'} \right) \frac{\partial (\ln A')}{\partial x'} \right] \\ & - u' \left[ \frac{\partial^2 \phi}{\partial x'^2} + \left( \frac{\partial V}{\partial x'} \right) \left( \frac{\partial \phi}{\partial x'} \right) \right] \end{aligned} \quad (9b)$$

### Vibrational Nonequilibrium

The present time-dependent analysis has been applied to the vibrational nonequilibrium expansion of a pure diatomic gas. These conditions are illustrative of many practical nozzle applications where the reservoir temperature is high enough to excite the vibrational energy mode, but not high enough to result in noticeable dissociation of the gas. In addition, the vibrational mode is assumed to be in equilibrium within itself but not in equilibrium with the translational and rotational modes; i.e., a Boltzmann distribution is assumed to exist within the vibrational mode. Consequently, a vibrational temperature  $T_{vib}$ , not necessarily equal to the translational temperature  $T$ , can be defined. With  $e = \frac{5}{2} RT + e_{vib}$ , equation (4) becomes

$$\frac{\partial T}{\partial t} = \frac{2}{5} \left[ -T \frac{\partial u}{\partial x} - T u \frac{\partial (\ln A)}{\partial x} - \frac{1}{R} \left( \frac{\partial e_{vib}}{\partial t} + u \frac{\partial e_{vib}}{\partial x} \right) \right] - u \frac{\partial T}{\partial x} \quad (10)$$

Defining  $e'_{vib} = e_{vib}/RT_0$  and  $\theta = \ln(e'_{vib})$ , the nondimensional form of equation (10) is

$$\frac{\partial \phi}{\partial t'} = -\frac{2}{5} \left( u' \frac{\partial V}{\partial x'} + u' \frac{\partial (\ln A')}{\partial x'} + \frac{e'_{\text{vib}}}{T'} \frac{\partial \theta}{\partial t'} + \frac{u' e'_{\text{vib}}}{T'} \frac{\partial \theta}{\partial x'} \right) - u' \frac{\partial \phi}{\partial x'} \quad (11)$$

In the rate equation, equation (5),  $q = e_{\text{vib}}$  and  $w$  is assumed to be the relaxation equation for a harmonic oscillator. Therefore, equation (5) becomes

$$\frac{\partial e_{\text{vib}}}{\partial t} = \frac{1}{\tau} [(e_{\text{vib}})_{\text{eq}} - e_{\text{vib}}] - u \frac{\partial e_{\text{vib}}}{\partial x} \quad (12)$$

where  $\tau$  is the vibrational relaxation time,  $\tau = f(p, T)$ , and  $(e_{\text{vib}})_{\text{eq}}$  is the equilibrium vibrational energy evaluated at the local translational temperature of the gas,  $(e_{\text{vib}})_{\text{eq}} = (h\nu/k)R/[\exp(h\nu/kT)-1]$ . Defining  $\tau' = \tau/(L/a_0)$ , the nondimensional form of equation (12) is

$$\frac{\partial \theta}{\partial t'} = \frac{1}{\tau'} \left[ \frac{(e'_{\text{vib}})_{\text{eq}}}{e'_{\text{vib}}} - 1 \right] - u' \frac{\partial \theta}{\partial x'} \quad (13)$$

Equations (11) and (13) directly yield  $(\frac{\partial g}{\partial t})_t$  for use in equation (1), where  $g = \phi$  and  $\theta$ . As usual, values for  $(\frac{\partial^2 g}{\partial t^2})$  and  $\frac{\partial^2 g}{\partial x \partial t}$  are obtained by differentiation of equations (11) and (13) with respect to  $t'$  and  $x'$  respectively

$$\begin{aligned} \frac{\partial^2 \phi}{\partial t'^2} = & -\frac{2}{5} \left[ u' \left( \frac{\partial^2 V}{\partial x' \partial t'} + \frac{\partial V}{\partial x'} \frac{\partial V}{\partial t'} + \frac{\partial (\ln A')}{\partial x'} \frac{\partial V}{\partial t'} \right) + \frac{e'_{\text{vib}}}{T'} \frac{\partial^2 \theta}{\partial t'^2} \right. \\ & + \frac{e'_{\text{vib}}}{T'} \left( \frac{\partial \theta}{\partial t'} \right) \left( \frac{\partial \theta}{\partial t'} - \frac{\partial \phi}{\partial t'} \right) + \frac{u' e'_{\text{vib}}}{T'} \frac{\partial^2 \theta}{\partial x' \partial t'} \\ & \left. + \frac{u' e'_{\text{vib}}}{T'} \frac{\partial \theta}{\partial x'} \left( \frac{\partial \theta}{\partial t'} + \frac{\partial V}{\partial t'} - \frac{\partial \phi}{\partial t'} \right) \right] - u' \left( \frac{\partial^2 \phi}{\partial x' \partial t'} + \frac{\partial \phi}{\partial x'} \frac{\partial V}{\partial t'} \right) \end{aligned} \quad (11a)$$

$$\begin{aligned}
 \frac{\partial^2 \phi}{\partial x' \partial t'} = & -\frac{2}{5} \left\{ u' \left[ \frac{\partial^2 V}{\partial x'^2} + \left( \frac{\partial V}{\partial x'} \right)^2 + \frac{\partial^2 (\ln A')}{\partial x'^2} + \frac{\partial (\ln A')}{\partial x'} \frac{\partial V}{\partial x'} \right] \right. \\
 & + \frac{e'_{\text{vib}}}{T'} \frac{\partial^2 \theta}{\partial x' \partial t'} + \frac{e'_{\text{vib}}}{T'} \frac{\partial \theta}{\partial t'} \left( \frac{\partial \theta}{\partial x'} - \frac{\partial \phi}{\partial x'} \right) + \frac{u' e'_{\text{vib}}}{T'} \frac{\partial^2 \theta}{\partial x'^2} \\
 & \left. + \frac{u' e'_{\text{vib}}}{T'} \frac{\partial \theta}{\partial x'} \left( \frac{\partial \theta}{\partial x'} + \frac{\partial V}{\partial x'} - \frac{\partial \phi}{\partial x'} \right) \right\} - u' \left( \frac{\partial^2 \phi}{\partial x'^2} + \frac{\partial \phi}{\partial x'} \frac{\partial V}{\partial x'} \right)
 \end{aligned} \quad (11b)$$

$$\begin{aligned}
 \frac{\partial^2 \theta}{\partial t'^2} = & \frac{1}{\tau'} \left[ \frac{1}{e'_{\text{vib}}} \frac{\partial (e'_{\text{vib}})_{\text{eq}}}{\partial t'} - \frac{(e'_{\text{vib}})_{\text{eq}}}{e'_{\text{vib}}} \frac{\partial \theta}{\partial t'} \right] - \frac{1}{(\tau')^2} \left[ \frac{(e'_{\text{vib}})_{\text{eq}}}{e'_{\text{vib}}} - 1 \right] \frac{\partial \tau'}{\partial t'} \\
 & - u' \left( \frac{\partial^2 \theta}{\partial x' \partial t'} + \frac{\partial \theta}{\partial x'} \frac{\partial V}{\partial t'} \right)
 \end{aligned} \quad (13a)$$

$$\begin{aligned}
 \frac{\partial^2 \theta}{\partial t' \partial x'} = & \frac{1}{\tau'} \left[ \frac{1}{e'_{\text{vib}}} \frac{\partial (e'_{\text{vib}})_{\text{eq}}}{\partial x'} - \frac{(e'_{\text{vib}})_{\text{eq}}}{e'_{\text{vib}}} \frac{\partial \theta}{\partial x'} \right] - \frac{1}{(\tau')^2} \left[ \frac{(e'_{\text{vib}})_{\text{eq}}}{e'_{\text{vib}}} - 1 \right] \frac{\partial \tau'}{\partial x'} \\
 & - u' \left( \frac{\partial^2 \theta}{\partial x'^2} + \frac{\partial \theta}{\partial x'} \frac{\partial V}{\partial x'} \right)
 \end{aligned} \quad (13b)$$

These additional differentiations introduce new terms such as  $\frac{\partial e'_{\text{vib}}}{\partial t'}$ ,  $\frac{\partial (e'_{\text{vib}})_{\text{eq}}}{\partial t'}$ ,  $\frac{\partial \tau'}{\partial t'}$ , and the corresponding  $x'$ -derivatives.

$$\frac{\partial e'_{\text{vib}}}{\partial t'} = e'_{\text{vib}} \frac{\partial \theta}{\partial t'}$$

$$\frac{\partial e'_{\text{vib}}}{\partial x'} = e'_{\text{vib}} \frac{\partial \theta}{\partial x'}$$

$$\frac{\partial (e'_{\text{vib}})_{\text{eq}}}{\partial t'} = \frac{\left( \frac{h\nu}{kT} \right)^2 (e^{h\nu/kT}) \frac{\partial \phi}{\partial t'} T'}{(e^{h\nu/kT} - 1)^2}$$

$$\frac{\partial (e'_{vib})_{eq}}{\partial x'} = \frac{(\frac{hv}{kT})^2 (e^{hv/kT}) \frac{\partial \phi}{\partial x'} T'}{(e^{hv/kT} - 1)^2}$$

If  $\tau$  is assumed to vary as  $\tau p = ae^{bT^C}$ , then

$$\frac{\partial \tau'}{\partial t'} = \tau' (bc T^C \frac{\partial \phi}{\partial t'} - \frac{\partial \phi}{\partial t'} - \frac{\partial Z}{\partial t'})$$

$$\frac{\partial \tau'}{\partial x'} = \tau' (bc T^C \frac{\partial \phi}{\partial x'} - \frac{\partial \phi}{\partial x'} - \frac{\partial Z}{\partial x'})$$

Finite-difference expressions for  $\frac{\partial \tau'}{\partial t'}$  and  $\frac{\partial \tau'}{\partial x'}$  can also be used, as discussed in a subsequent section.

Initial values at  $t = 0$  are assumed for  $\rho$ ,  $u$  and  $T$ . For convenience, the initial values for  $e_{vib}$  in the subsonic and throat regions are equilibrium values at the local assumed  $T$ , whereas at some arbitrary point downstream of the throat  $e_{vib}$  is usually set equal to a constant for the remainder of the nozzle. Consequently, the initial  $e_{vib}$  distribution is at least qualitatively similar to the actual steady-state nonequilibrium distribution.

#### Chemical Nonequilibrium

The present time-dependent analysis has also been applied to the case of a nonequilibrium dissociating symmetrical diatomic gas



where  $M_j$  is a collision partner (catalytic body); in the present application,  $M_1 = A_2$  and  $M_2 = A$ . Also, chemical nonequilibrium

is the only rate process considered; the vibrational energy is assumed to be in equilibrium with translation and rotation at the local gas temperature. Hence, for simplicity, no attempt is made to account for coupling between vibration and dissociation, even though such coupling effects may be important in some practical applications.<sup>1</sup> Letting subscript  $i$  denote a given chemical species,  $e = \sum_i \eta_i E_i$ , where  $\eta_i$  is the mole-mass ratio<sup>15</sup> (moles of species  $i$  per unit mass of mixture),  $E_i$  is the molar internal energy of species  $i$  including its heat of formation, and  $dE_i = C_{v_i} dT$ . Also, the local frozen specific heat per unit mass of the mixture is  $c_{v_f} = \sum_i \eta_i C_{v_i}$ , and the local value of the specific gas constant is  $R = \sum_i \eta_i R_i$ . In terms of the above quantities, equations (3) and (4) become

$$\rho \frac{\partial u}{\partial t} + \rho u \frac{\partial u}{\partial x} = -(\rho R \frac{\partial T}{\partial x} + T \rho \frac{\partial R}{\partial x} + TR \frac{\partial \rho}{\partial x}) \quad (15)$$

$$\frac{\partial T}{\partial t} = -\left(\frac{RT}{c_{v_f}}\right) \left(\frac{\partial u}{\partial x} + u \frac{\partial \ln A}{\partial x}\right) - u \frac{\partial T}{\partial x} - \frac{u}{c_{v_f}} \sum_i E_i \frac{\partial \eta_i}{\partial x} - \frac{1}{c_{v_f}} \sum_i E_i \frac{\partial \eta_i}{\partial t} \quad (16)$$

and equation (5) becomes

$$\frac{\partial \eta_i}{\partial t} = \dot{w}_i - u \frac{\partial \eta_i}{\partial x} \quad (17)$$

where  $w_i$  is the rate of production of species  $i$  by internal chemical reactions. Defining  $\eta_i' = \eta_i/\eta_0$ ,  $E_i' = E_i/E_0$  and  $\Gamma_i = \ln \eta_i'$ , where  $\eta_0$  and  $E_0$  are the reservoir values of the mixture mole-mass ratio and molar internal energy respectively, nondimensional forms of equations (15), (16) and (17) are obtained as

$$\frac{\partial V}{\partial t'} = -u' \frac{\partial V}{\partial x'} - \frac{T'}{\gamma_o u'} \left[ \frac{R}{R_o} \frac{\partial \phi}{\partial x'} + \frac{\partial (R/R_o)}{\partial x'} + \frac{R}{R_o} \frac{\partial Z}{\partial x'} \right] \quad (18)$$

$$\frac{\partial \phi}{\partial t'} = - \frac{R}{c_{vf}} u' \left( \frac{\partial V}{\partial x'} + \frac{\partial \ln A'}{\partial x'} \right) - u' \frac{\partial \phi}{\partial x'} - \left( \frac{E_o \eta_o}{T_o} \right) \left( \frac{1}{c_{vf} T'} \right) \sum_i E_i' \dot{w}_i' \quad (19)$$

and

$$\frac{\partial \Gamma_i}{\partial t'} = \frac{\dot{w}_i'}{\eta_i'} - u' \frac{\partial \Gamma_i}{\partial x'} \quad (20)$$

where, for the atomic species

$$\begin{aligned} \dot{w}_i' = \dot{w}_A' = & \left( \frac{L \rho_o \eta_o}{a_o} \right) \rho' [k_F^{(1)} (\eta_{A_2}')^2 + k_F^{(2)} (\eta_{A_2}') (\eta_A')] \\ & - \left( \frac{L \rho_o^2 \eta_o^2}{a_o} \right) (\rho')^2 [k_R^{(1)} (\eta_A')^2 (\eta_{A_2}') + k_R^{(2)} (\eta_A')^3] \end{aligned} \quad (21)$$

Note that the appearance of  $\gamma_o$  in equation (18) is strictly due to the arbitrary choice of  $a_o = (\gamma_o R_o T_o)^{1/2}$  as a nondimensionalizing quantity;  $\gamma_o$  is the ratio of the frozen specific heats evaluated at reservoir conditions and has no other significance in the present formulation for a nonequilibrium chemically reacting gas.

Equations (18) through (21) directly yield  $\left( \frac{\partial g}{\partial t} \right)_t$  for use in equation (1) where  $g = V, \phi$  and  $\Gamma_i$ ;  $\left( \frac{\partial^2 g}{\partial t^2} \right)_t$  and  $\frac{\partial^2 g}{\partial t \partial x}$  are obtained by differentiation of equations (18) through (20) with respect to  $t'$  and  $x'$  respectively.

$$\begin{aligned} \frac{\partial^2 V}{\partial t'^2} = & - u' \left( \frac{\partial^2 V}{\partial x' \partial t'} + \frac{\partial V}{\partial x'} \frac{\partial V}{\partial t'} \right) - \frac{T'}{\gamma_o u'} \left[ G \frac{\partial^2 \phi}{\partial x' \partial t'} + \frac{\partial \phi}{\partial x'} \frac{\partial G}{\partial t'} + \frac{\partial^2 G}{\partial x' \partial t'} \right. \\ & \left. + G \frac{\partial^2 Z}{\partial x' \partial t'} + \frac{\partial Z}{\partial x'} \frac{\partial G}{\partial t'} + \left( G \frac{\partial \phi}{\partial x'} + \frac{\partial G}{\partial x'} + G \frac{\partial Z}{\partial x'} \right) \left( \frac{\partial \phi}{\partial t'} - \frac{\partial V}{\partial t'} \right) \right] \end{aligned} \quad (18a)$$

$$\begin{aligned} \frac{\partial^2 V}{\partial x'^2 \partial t'} = & -u' \left[ \frac{\partial^2 V}{\partial x'^2} + \left( \frac{\partial V}{\partial x'} \right)^2 \right] - \frac{T'}{\gamma_O u'} \left[ G \frac{\partial^2 \phi}{\partial x'^2} + \frac{\partial \phi}{\partial x'} \frac{\partial G}{\partial x'} + \frac{\partial^2 G}{\partial x'^2} \right. \\ & \left. + G \frac{\partial^2 Z}{\partial x'^2} + \frac{\partial Z}{\partial x'} \frac{\partial G}{\partial x'} + \left( \frac{\partial \phi}{\partial x'} - \frac{\partial V}{\partial x'} \right) \left( G \frac{\partial \phi}{\partial x'} + \frac{\partial G}{\partial x'} + G \frac{\partial Z}{\partial x'} \right) \right] \end{aligned} \quad (18b)$$

$$\text{where } G = R/R_O = \eta_O \eta_O (\eta_A' + \eta_{A_2}')$$

$$\begin{aligned} \frac{\partial^2 \phi}{\partial t'^2} = & - \left( \frac{R}{c_{vf}} \right) u' \left[ \frac{\partial^2 V}{\partial x'^2 \partial t'} + \left( \frac{\partial V}{\partial x'} + \frac{\partial \ln A'}{\partial x'} \right) \frac{\partial V}{\partial t'} \right] \\ & - u' \left( \frac{\partial V}{\partial x'} + \frac{\partial \ln A'}{\partial x'} \right) \left[ \frac{1}{c_{vf}} \frac{\partial R}{\partial t'} - \frac{R}{(c_{vf})^2} \frac{\partial c_{vf}}{\partial t'} \right] - u' \left( \frac{\partial^2 \phi}{\partial x'^2 \partial t'} + \frac{\partial \phi}{\partial x'} \frac{\partial V}{\partial t'} \right) \\ & - \left( \frac{E_O \eta_O}{T_O} \right) \left( \frac{1}{c_{vf} T'} \right) \left[ \Sigma_i \left( E_i' \frac{\partial \dot{w}_i'}{\partial t'} + \dot{w}_i' \frac{\partial E_i'}{\partial t'} \right) - \left( \frac{\partial \phi}{\partial t'} + \frac{1}{c_{vf}} \frac{\partial c_{vf}}{\partial t'} \right) (\Sigma_i E_i' \dot{w}_i') \right] \end{aligned} \quad (19a)$$

$$\begin{aligned} \frac{\partial^2 \phi}{\partial x'^2 \partial t'} = & - \left( \frac{R}{c_{vf}} \right) u' \left[ \frac{\partial^2 V}{\partial x'^2} + \frac{\partial^2 \ln A'}{\partial x'^2} + \left( \frac{\partial V}{\partial x'} + \frac{\partial \ln A'}{\partial x'} \right) \frac{\partial V}{\partial x'} \right] \\ & - u' \left( \frac{\partial V}{\partial x'} + \frac{\partial \ln A'}{\partial x'} \right) \left[ \left( \frac{1}{c_{vf}} \right) \frac{\partial R}{\partial x'} - \frac{R}{(c_{vf})^2} \frac{\partial c_{vf}}{\partial x'} \right] - u' \left( \frac{\partial^2 \phi}{\partial x'^2} + \frac{\partial \phi}{\partial x'} \frac{\partial V}{\partial x'} \right) \\ & - \left( \frac{E_O \eta_O}{T_O} \right) \left( \frac{1}{c_{vf} T'} \right) \left[ \Sigma_i \left( E_i' \frac{\partial \dot{w}_i'}{\partial x'} + \dot{w}_i' \frac{\partial E_i'}{\partial x'} \right) - (\Sigma_i E_i' \dot{w}_i') \left( \frac{\partial \phi}{\partial x'} + \frac{1}{c_{vf}} \frac{\partial c_{vf}}{\partial x'} \right) \right] \end{aligned} \quad (19b)$$

$$\frac{\partial^2 \Gamma_i}{\partial t'^2} = \frac{1}{\eta_i'} \left( \frac{\partial \dot{w}_i'}{\partial t'} - \dot{w}_i' \frac{\partial \Gamma_i}{\partial t'} \right) - u' \left( \frac{\partial^2 \Gamma_i}{\partial x'^2 \partial t'} + \frac{\partial \Gamma_i}{\partial x'} \frac{\partial V}{\partial x'} \right) \quad (20a)$$

$$\frac{\partial^2 \Gamma_i}{\partial x'^2 \partial t'} = \frac{1}{\eta_i'} \left( \frac{\partial \dot{w}_i'}{\partial x'} - \dot{w}_i' \frac{\partial \Gamma_i}{\partial x'} \right) - u' \left( \frac{\partial^2 \Gamma_i}{\partial x'^2} + \frac{\partial \Gamma_i}{\partial x'} \frac{\partial V}{\partial x'} \right) \quad (20b)$$

These differentiations introduce new terms such as  $\frac{\partial \dot{w}_A'}{\partial t'}$ ,  $\frac{\partial k_R^j}{\partial t'}$ ,  $\frac{\partial R}{\partial t'}$ ,  $\frac{\partial c_{vf}}{\partial t'}$ ,  $\frac{\partial E_i}{\partial t'}$ , as well as the corresponding  $x'$ -derivatives. Straightforward but somewhat lengthy expressions for these terms are derived as follows.

$$\begin{aligned} \frac{\partial \dot{w}_A'}{\partial t'} = & \left( \frac{L \rho_o \eta_o}{a_o} \right) \rho' \left\{ 2k_F^{(1)} \eta_{A_2}' \frac{\partial \eta_{A_2}'}{\partial t'} + (\eta_{A_2}')^2 \frac{\partial k_F^{(1)}}{\partial t'} \right. \\ & + k_F^{(2)} \left( \eta_{A_2}' \frac{\partial \eta_A'}{\partial t'} + \eta_A' \frac{\partial \eta_{A_2}'}{\partial t'} \right) + \eta_{A_2}' \eta_A' \frac{\partial k_F^{(2)}}{\partial t'} \\ & + [k_F^{(1)} (\eta_{A_2}')^2 + k_F^{(2)} (\eta_{A_2}') (\eta_A')] \frac{\partial Z}{\partial t'} \left\{ \right. \\ & - \left[ \frac{L (\rho_o \eta_o)^2}{a_o} \right] (\rho')^2 \left\{ k_R^{(1)} [(\eta_A')^2 \frac{\partial \eta_{A_2}'}{\partial t'} + 2 \eta_{A_2}' \eta_A' \frac{\partial \eta_A'}{\partial t'}] \right. \\ & + (\eta_A')^2 (\eta_{A_2}') \frac{\partial k_R^{(1)}}{\partial t'} + 3 k_R^{(2)} (\eta_A')^2 \frac{\partial \eta_A'}{\partial t'} + (\eta_A')^3 \frac{\partial k_R^{(2)}}{\partial t'} \\ & \left. \left. + 2 [k_R^{(1)} (\eta_A')^2 (\eta_{A_2}') + k_R^{(2)} (\eta_A')^3] \frac{\partial Z}{\partial t'} \right\} \right. \end{aligned}$$

$$\frac{\partial R}{\partial t'} = R \eta_o \left( \frac{\partial \eta_A'}{\partial t'} + \frac{\partial \eta_{A_2}'}{\partial t'} \right)$$

$$\frac{\partial c_{vf}}{\partial t'} = c_{vA} \eta_o \frac{\partial \eta_A'}{\partial t'} + \eta_o \eta_{A_2}' \frac{\partial c_{vA_2}}{\partial t'} + c_{vA_2} \eta_o \frac{\partial \eta_{A_2}'}{\partial t'}$$

where

$$c_{vA_2} = \frac{5}{2} R + \left[ \frac{\left( \frac{h\nu}{kT} \right)^2 e^{h\nu/kT}}{(e^{h\nu/kT} - 1)^2} \right] R$$

$$c_{vA} = \frac{3}{2} R$$



$$\frac{\partial E_A'}{\partial t'} = \frac{3}{2} R \frac{T_O}{E_O} T' \frac{\partial \phi}{\partial t'}$$

$$\frac{\partial E_{A_2}'}{\partial t'} = R \frac{T_O}{E_O} T' \frac{\partial \phi}{\partial t'} \left[ \frac{5}{2} + \frac{\left(\frac{h\nu}{kT}\right)^2 e^{h\nu/kT}}{(e^{h\nu/kT}-1)^2} \right]$$

In the above, the electronic energy of each species has been assumed negligibly small in comparison to the translational, rotational and vibrational energy. This is a reasonable assumption for the temperature range considered in the present results.

Following Reference 2, the reverse reaction rate constants  $k_R^{(1)}$  and  $k_R^{(2)}$  are assumed to vary as

$$k_R^{(1)} = k_{R_O}^{(1)} (T')^{-s}$$

$$k_R^{(2)} = 35 (T'/T_D') k_R^{(1)}$$

$$\frac{\partial k_R^{(1)}}{\partial t'} = -s k_{R_O}^{(1)} (T')^{-s} \frac{\partial \phi}{\partial t'}$$

$$\frac{\partial k_R^{(2)}}{\partial t'} = 35 \frac{T'}{T_D'} \left( \frac{\partial k_R^{(1)}}{\partial t'} + k_R^{(1)} \frac{\partial \phi}{\partial t'} \right)$$

Note that  $\frac{\partial k_R^{(2)}}{\partial t'} = 0$  when  $s = 1$ . Also, the forward reaction rate constants and their derivatives are obtained from the relation  $k_F/k_R = K_e(T)$ , where  $K_e(T)$  is the equilibrium constant.

Initial conditions at  $t = 0$  are assumed for  $\rho$ ,  $u$ , and  $T$ . The initial distribution for  $\eta_A$  in the subsonic and throat regions is obtained from a chemical equilibrium calculation using the local assumed initial distributions of  $\rho$  and  $T$ , whereas at some arbitrary

point downstream of the throat,  $\eta_A$  is set equal to a constant for the remainder of the nozzle. Consequently, in the same vein as the vibrational nonequilibrium case, the initial  $\eta_A$  distribution is at least qualitatively similar to the actual steady-state nonequilibrium distribution.

#### Comments on the Numerical Solution

Several comments are in order regarding the numerical behavior of the present time-dependent method. First, in equations (7), (8), (9), (11), (13), (18), (19) and (20), the  $x'$ -derivatives are computed from central differences

$$\frac{\partial g}{\partial x'} = \frac{g(x' + \Delta x') - g(x' - \Delta x')}{2\Delta x'}$$

$$\frac{\partial^2 g}{\partial x'^2} = \frac{g(x' + \Delta x') - 2g(x') + g(x' - \Delta x')}{(\Delta x')^2}$$

evaluated from the known flow field at time  $t'$ . Second, the initial conditions appear to have no meaningful effect upon either the stability or convergence of the technique; results have been obtained for identical nozzles and reservoir conditions but with widely different initial conditions, and in each case the same steady-state solution was obtained. Also, second-order accuracy as embodied in equation (1) appears to be absolutely necessary for stability. Several attempts at first-order accuracy (using the first two terms in equation (1)) met with instabilities for both the calorically perfect gas and the nonequilibrium cases. Hence, the second-order term involving  $\frac{\partial^2 g}{\partial t^2}$  in equation (1) is apparently necessary for convergence.

Regarding the vibrational nonequilibrium case, the nonequilibrium expansion of a mixture of gases may result in complicated expressions for  $\tau$  as compared to the relatively simple variation assumed above. Consequently, analytical expressions for  $\frac{\partial \tau'}{\partial t'}$  and  $\frac{\partial \tau'}{\partial x'}$  as presented above may be extremely tedious, if possible at all. However, experience with the present analysis has shown that these derivatives can be approximated directly by the finite-difference expressions

$$\left(\frac{\partial \tau'}{\partial t'}\right)_{t'} = \frac{(\tau')_{t'} - (\tau')_{(t' - \Delta t')}}{\Delta t'}$$

$$\left(\frac{\partial \tau'}{\partial x'}\right)_{t'} = \left[ \frac{\tau'(x' + \Delta x') - \tau'(x' - \Delta x')}{2\Delta x'} \right]_{t'}$$

evaluated from the known flow field at times  $t'$  and  $(t' - \Delta t')$ .

The use of these finite-difference expressions instead of analytical forms for  $\frac{\partial \tau'}{\partial t'}$  and  $\frac{\partial \tau'}{\partial x'}$  results in less than a 0.2 percent change in the final steady-state values for  $e_{vib}$  through the nozzle, and no noticeable change at all in the other nozzle flow variables.

The time increment  $\Delta t$  appearing in equation (1) is chosen at the end of each time step to satisfy both the Courant-Friedrichs-Lewy stability criterion, where

$$\Delta t' \leq \frac{\Delta x'}{u' + a'} \quad (22)$$

and a criterion geared to the speed of the nonequilibrium relaxation process

$$\Delta t' < B\psi \quad (23)$$

where  $\Psi = \tau'$  for vibrational nonequilibrium,  $\Psi = \frac{\partial \dot{w}'_A}{\partial \eta_A}$  for chemical nonequilibrium,<sup>15</sup> and B is a proportionality constant, found empirically to be approximately 0.2 for the present investigation. Both criteria must be satisfied simultaneously because two "relaxation" processes prevail in the time-dependent flow as it progresses towards the steady-state; a fluid dynamic relaxation (eq. (22)) involving the propagation and interaction of compression and expansion waves throughout the nozzle, and an internal physical-chemical relaxation (eq. (23)) involving the finite rate processes of vibrational energy and chemical composition changes.

Because of the central differences employed in the present analysis, the flow-field variables at the first and last points in the grid (see Figure 1) can not be directly obtained from equation (1). Instead, at the last point (nozzle exit) all the flow properties (in terms of  $Z$ ,  $V$ ,  $\phi$ , etc.) are simply obtained from linear extrapolation from the two previous internal points. The first grid point (nozzle inlet) is considered to be effectively in the reservoir, i.e.,  $A/A^*$  at this point is a large number, usually greater than ten. Hence, values of  $p$ ,  $T$  and  $\rho$  at this point are assumed to be reservoir values and held fixed, invariant with time. The flow velocity (in terms of  $V$ ) at this point is allowed to vary with time, and is found by linear extrapolation from the second and third internal points. At large values of time, the velocity at the inlet approaches its proper steady-state value (a very small but finite number), compatible with the proper steady-state mass flow through the nozzle.

As a general comment, the philosophy of the present analysis is similar to the time-dependent solutions of the supersonic blunt-body problem presented in References 16 and 17. Because the unsteady gas-dynamic conservation equations are hyperbolic with respect to time, the time-dependent method is admirably suited for the unified analysis of mixed subsonic-supersonic flow fields. Indeed, the expansion through a convergent-divergent nozzle is such a case.

#### RESULTS

Using the present time-dependent analysis, numerical results have been obtained on an IBM 7090 digital computer for the three cases of a calorically perfect gas, vibrational nonequilibrium expansion of diatomic nitrogen, and the chemical nonequilibrium expansion of partially dissociated oxygen. Again, emphasis is made that the desired results are the steady-state flow fields, and that the present time-dependent analysis is an advantageous means to that end. As schematically shown in Figure 1, the computations are made at equally spaced grid points along the nozzle. As few as 30 grid points are employed in a calculation; this is a convenient number and does not represent a required minimum for stability. Indeed, a virtue of the present time-dependent analysis is that relatively large spacings between grid points can be employed throughout the nozzle, including the near equilibrium subsonic region near the reservoir. In addition, using the present time-dependent analysis for the case of vibrational nonequilibrium, several numerical experiments have been performed to examine the

effect of the shape (area distribution) of the subsonic nozzle section on the resulting frozen vibrational energy at the nozzle exit. For some practical reservoir conditions, the results show a noticeable effect, as will be discussed in a subsequent section.

#### Calorically Perfect Gas

In order to investigate the purely fluid dynamic behavior of the present time-dependent analysis, results have been obtained for a calorically perfect gas with  $\gamma = 1.4$ ; some of these results are illustrated in Figures 2 to 4. Starting with an initial linear distribution, the transient profiles of  $T'$  through the nozzle are shown at various time steps in Figure 2. Two important points are noted from Figure 2: (1) At early values of time, the profiles relax very rapidly to a steady-state distribution, and (2) the resulting steady-state distribution shows excellent agreement with known steady-state results obtained from Reference 18. These results are complemented by the transient profiles of local mass flow,  $\rho uA$ , through the nozzle, as shown in Figure 3. The somewhat wavy initial distribution for  $\rho uA$  is a consequence of the arbitrarily assumed initial distributions for  $\rho$  and  $u$ . Figure 3 markedly illustrates that the transient solution rapidly proceeds to the proper steady mass flow,  $\rho uA = \text{constant}$ . This aspect of the present analysis is an important virtue when applied to nonequilibrium flows, as described in the following sections. Excellent agreement for the steady-state distributions of  $p$  and  $u$  is also obtained, as shown in Figure 4.

Vibrational Nonequilibrium

Figures 5 to 9 illustrate results obtained with the present time-dependent analysis for the vibrational nonequilibrium expansion of  $N_2$ . For these results, the characteristic vibrational relaxation time was assumed to vary as  $\tau_p = a[\exp(-bT^{1/3})]$ , following Reference 11. With one exception, the present results are obtained with  $a = 14.7$  and  $b = 0.915$ , where  $p$  is in atm,  $T$  in  $^{\circ}K$ , and  $\tau$  in seconds. These values for  $a$  and  $b$  are fitted to the vibrational relaxation times used in References 8 and 13, which reflect the shock-tube data of Blackman.<sup>19</sup> Of course, recent experiments have shown that vibrational relaxation times measured behind normal shock waves and subsequently used in equation (12) are not appropriate for expanding flows,<sup>1,20</sup> however, this does not detract from the present results, which are intended to illustrate the present time-dependent analysis and which are compared with earlier analyses using Blackman's shock-tube data.

To illustrate the time-dependent behavior of the vibrational nonequilibrium solution, Figure 5 shows the transient  $e_{vib}$  profiles at various time steps; as in the previous case, a rapid approach to the steady-state distribution is observed. This steady-state distribution agrees with the results of a recent steady-flow analysis by Wilson et al,<sup>13</sup> as shown in terms of  $T_{vib}$  in Figure 6. Both the present time-dependent analysis and the steady-flow analysis of Reference 13 include nonequilibrium effects upstream of the throat. The comparisons in Figure 6 are made for several reservoir temperatures, and show very good agreement between the time-dependent and steady-flow approaches; however, emphasis is

again made that the present time-dependent results were obtained in a straightforward manner, whereas the steady-flow analysis of Wilson et al requires an iterative procedure as well as a forward integration matched to an expansion about a singular point slightly downstream of the throat.

For some practical reservoir conditions, nonequilibrium effects upstream of the throat are noticeable and have a subsequent influence on the frozen vibrational energy at the nozzle exit; these effects are shown in Figures 7 to 9. Figure 7 compares results for distributions of  $T_{vib}$  and  $T_{trans}$  obtained with the present time-dependent analysis, which includes nonequilibrium effects upstream of the throat, with the results obtained with a steady-flow analysis by Harris and Albacete,<sup>7</sup> which assumes local thermodynamic equilibrium from the reservoir to the throat. For this comparison, the constants in  $\tau_p = a[\exp(-bT^{1/3})]$  are  $a = 0.077$  and  $b = 0.576$ , which are fitted to the quantum mechanical calculations of Widom.<sup>21</sup> Two important points are obtained from the comparison shown in Figure 7: (1) the present results show a noticeable departure from equilibrium flow upstream of the throat as reflected by the difference between  $T_{trans}$  and  $T_{vib}$  and (2) these upstream nonequilibrium effects result in a higher frozen  $T_{vib}$  at the nozzle exit in comparison to the results of Reference 7. For the reservoir conditions shown in Figure 7, the vibrational energy is a relatively small fraction of the internal energy of the gas. Hence, the differences in  $T_{vib}$  between the two analyses are not paralleled by similar differences in  $T_{trans}$ ; indeed, good agreement



is obtained for  $T_{trans}$ . In addition, good agreement is also obtained for  $p$  and  $u$  as shown in Figure 8. The upstream nonequilibrium effects are accentuated at lower pressures, as markedly shown in Figure 9. Here, the present results are compared with the steady-state analysis of Erickson,<sup>8</sup> which like that of Reference 7 assumes equilibrium flow to the throat. The results, which are given in terms of local nonequilibrium vibrational energy non-dimensionalized by the reservoir equilibrium value, again illustrate the effect of nonequilibrium conditions upstream of the throat, particularly for the lower value of  $p_0$ . Consequently, Figures 7 and 9 demonstrate the importance of treating nonequilibrium effects upstream of the throat when solving the nonequilibrium nozzle flow problem. In contrast to a steady-flow approach, the present time-dependent analysis handles such effects in a straightforward manner.

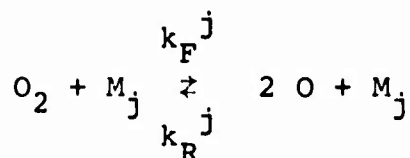
#### Influence of Subsonic Area Distribution

The fact that significant nonequilibrium conditions can prevail upstream of the throat prompts the following question: What is the effect of the shape (area distribution) of the subsonic section on the resulting frozen vibrational energy at the nozzle exit? In order to examine this question, several numerical experiments have been performed using the present time-dependent technique. Figures 10 and 11 reflect some results from these experiments in which vibrational temperature distributions are compared for two nozzles with different subsonic sections but identical supersonic sections. These nozzles are shown schematically

in Figure 10; the composite nozzle exhibits a greater subsonic area change near the throat than the purely hyperbolic nozzle. Figure 10 shows only a small difference in frozen  $T_{vib}$  at the nozzle exit for a reservoir pressure of 80 atm. However, Figure 11 shows that at a lower pressure of 10 atm a considerable difference in frozen vibrational temperature is obtained and this difference appears to be relatively insensitive to the reservoir temperature. Consequently, for practical reservoir conditions, some tailoring of the frozen vibrational energy at the nozzle exit can be accomplished by proper design of the subsonic section.

#### Chemical Nonequilibrium

Figures 12 to 17 illustrate results obtained with the present time-dependent analysis for the case of the chemical nonequilibrium expansion of partially dissociated oxygen



where  $M_1 = O_2$  and  $M_2 = O$ . The reaction rate constants and nozzle shape are taken identical to those of Hall and Russo,<sup>1,2</sup> where  $k_R^{(1)} = k_{R_O}^{(1)} (T_O/T)$ ,  $k_R^{(2)}/k_R^{(1)} = 35 T/T_D$ ,  $T_D = D/k$ ,  $D$  is the dissociation energy per molecule, and  $k_F^j/k_R^j = K_e$ . For the present results, the equilibrium constant,  $K_e$ , is obtained from Wray<sup>22</sup> as  $K_e = (1.2 \times 10^3) T^{-1/2} \exp(-118,000/RT)$ , where  $K_e$  is in moles/cm<sup>3</sup> and  $T$  in °K. Also in the present results the vibrational energy is assumed to be in the local thermodynamic equilibrium at the local gas temperature.

Figure 12 illustrates the transient profiles of atom mass fraction  $\alpha$  at various time steps, where  $\alpha = \rho_i/\rho = \eta_i m_i$ . As in the previous cases, a continuous approach to the steady state is observed. However, in comparison with Figures 2 and 5 from the previous cases, Figure 12 shows that the steady state for the chemical nonequilibrium case is obtained after considerably more time steps. This behavior is due to the small values of  $\Delta t$  dictated by equation (23) for the present chemical nonequilibrium conditions; this contrasts to the previous results for the calorically perfect gas and vibrational nonequilibrium cases, where the minimum  $\Delta t$  came from equation (22) and where the values of  $\Delta t$  were an order of magnitude larger than the present chemical nonequilibrium case. Also in Figure 12, the resulting steady-state distribution is compared to the results obtained from the steady-flow analysis by Hall and Russo;<sup>2</sup> very good agreement is obtained. (Note that a slight discrepancy occurs with the equilibrium reservoir mass fraction,  $\alpha_0$ , which can be attributed to slight differences in  $K_e$  between the two sets of results.)

Whereas the results shown in Figure 12 are computed for  $p_0 = 9.4$  atm, Figures 13 to 17 show results obtained for  $p_0 = 82$  atm, where equilibrium conditions are more closely approached, hence providing a more stringent test for the stability of a nonequilibrium flow analysis. Figure 13 shows the variation of  $\alpha$  at the nozzle exit as a function of time; the steady-state  $\alpha_{\text{exit}}$  is approached at large values of time. Figures 14 to 17 show results obtained with the present time-dependent analysis

for the steady-state  $\alpha$ ,  $T$ ,  $\rho$  and  $p$  distributions, respectively (plotted versus nozzle area ratio). These results are compared with the results of Hall and Russo, obtained from a steady-flow analysis. Very good agreement is obtained; however, emphasis is again made that the present results are obtained in a straightforward manner, whereas the steady-state analysis of Reference 2 requires an iterative procedure due to the unknown critical mass flow, and employs an asymptotic series solution for the flow at large areas upstream of the throat for starting the forward integration.

#### CONCLUSIONS

In summary, the following conclusions are made: (1) A new, alternative solution for quasi-one-dimensional nonequilibrium nozzle flows is presented. A virtue of this new technique is its simplicity, which prevails from its initial physical formulation to the successful receipt of numerical results. Consequently, the time-dependent technique appears to warrant consideration for future applications in nonequilibrium nozzle flows. (2) Because in some practical cases nonequilibrium conditions prevail upstream of the throat, the shape of the subsonic section can have a noticeable effect on the frozen vibrational energy at the nozzle exit.

Parenthetically, it should be noted that the present time-dependent results always converged to the supersonic solution downstream of the throat; a purely subsonic solution was never observed. This situation was due to the choice of initial values

NOLTR 69-52

which were in qualitative agreement with a supersonic solution (i.e., low exit values of density and temperature, and high values of velocity).

REFERENCES

1. Hall, J. G. and Treanor, C. E., "Nonequilibrium Effects in Supersonic Nozzle Flows," CAL No. 163, Mar 1968, Cornell Aeronautical Laboratory, Inc. (Also to appear as AGARD-ograph No. 124)
2. Hall, J. G. and Russo, A. L., "Studies of Chemical Nonequilibrium in Hypersonic Nozzle Flows," AFOSR TN 59-1090, CAL Report AD-1118-A-6, Nov 1959
3. Eschenroeder, A. Q., Boyer, D. W. and Hall, J. G., "Nonequilibrium Expansions of Air with Coupled Chemical Reactions," The Physics of Fluids, Vol 5, No. 5, May 1962, pp 615-624
4. Eschenroeder, A. Q., Boyer, D. W. and Hall, J. G., "Exact Solutions for Nonequilibrium Expansions of Air with Coupled Chemical Reactions," AFOSR 622, CAL Report AF-1413-A-1, May 1961
5. Lordi, J. A. and Mates, R. E., "Nonequilibrium Expansions of High-Enthalpy Airflows," ARL 64-206, Nov 1964
6. Mates, R. E. and Lordi, J. A., "Techniques for Solving Nonequilibrium Expanding Flow Problems," ARL 65-2, Jan 1965
7. Harris, E. L. and Albacete, L. M., "Vibrational Relaxation of Nitrogen in the NOL Hypersonic Tunnel No. 4," NOLTR 63-221, Apr 1964, U. S. Naval Ordnance Laboratory, White Oak, Maryland
8. Erickson, W. D., "Vibrational Nonequilibrium Flow of Nitrogen in Hypersonic Nozzles," NASA TN D-1810, Jun 1963
9. Stollery, J. L. and Smith, J. E., "A Note on the Variation of Vibrational Temperature Along a Nozzle," Journal of Fluid Mechanics, Vol 13, 1962, pp 225-236
10. Stollery, J. L. and Park, C., "Computer Solutions to the Problem of Vibrational Relaxation in Hypersonic Nozzle Flows," Imperial College of Science and Technology, Report No. 115, Jan 1963
11. Vincenti, W. G., "Calculations of the One-Dimensional Nonequilibrium Flow of Air Through a Hypersonic Nozzle - Interim Report," AEDC-TN-61-65, May 1961
12. Emanuel, G. and Vincenti, W. G., "Method for Calculation of the One-Dimensional Nonequilibrium Flow of a General Gas Mixture Through a Hypersonic Nozzle," AEDC-TDR-62-131, Jun 1962

13. Wilson, J. L., Schofield, D. and Lapworth, K. C., "A Computer Program for Non-Equilibrium Convergent-Divergent Nozzle Flow," National Physical Laboratory Report 1250, Aeronautical Research Council No. A.R.C. 29246, October 1967
14. Liepmann, H. W. and Roshko, A., Elements of Gasdynamics, John Wiley and Sons, New York, 1957
15. Vincenti, W. G. and Kruger, C. H., Jr., Introduction to Physical Gas Dynamics, John Wiley and Sons, New York, 1965, p 236
16. Anderson, J. D., Jr., Albacete, L. M. and Winkelmann, A. E., "On Hypersonic Blunt Body Flow Fields Obtained with a Time-Dependent Technique," NOLTR 68-129, U. S. Naval Ordnance Laboratory, White Oak, Md., Aug 1968
17. Moretti, G. and Abbett, M., "A Time-Dependent Computational Method for Blunt Body Flows," AIAA Journal, Vol 4, No. 12, Dec 1966, pp 2136-2141
18. Ames Research Staff, "Equations, Tables, and Charts for Compressible Flow," NACA Report 1135, 1953
19. Blackman, V. H., "Vibrational Relaxation in Oxygen and Nitrogen," Journal of Fluid Mechanics, Vol 1, Pt. 1, May 1956, pp 61-85
20. Hurle, I. R., Russo, A. L., and Hall, J. G., "Spectroscopic Studies of Vibrational Nonequilibrium in Supersonic Nozzle Flows," Journal of Chemical Physics, Vol 40, No. 8, Apr 1964 pp 2076-2089
21. Widom, B., "Inelastic Molecular Collisions with a Maxwellian Interaction Energy," Journal of Chemical Physics, Vol 27, Oct 1957, pp 940-952
22. Wray, K. L., "Chemical Kinetics of High Temperature Air," Hypersonic Flow Research, Academic Press, New York, 1962, pp 181-204
23. Pearson, W. E., "Channel Flow of Gaseous Mixtures in Chemical and Thermodynamic Nonequilibrium," The Physics of Fluids, Vol. 10, No. 11, Nov 1967, pp 2305-2311
24. Moretti, G., "A New Technique for the Numerical Analysis of Nonequilibrium Flows," AIAA Journal, Vol. 3, No. 2, Feb 1965, pp 223-229
25. Lomax, H. and Bailey, H. E., "A Critical Analysis of Various Numerical Integration Methods for Computing the Flow of a Gas in Chemical Nonequilibrium," NASA TN D-4109, Aug 1967

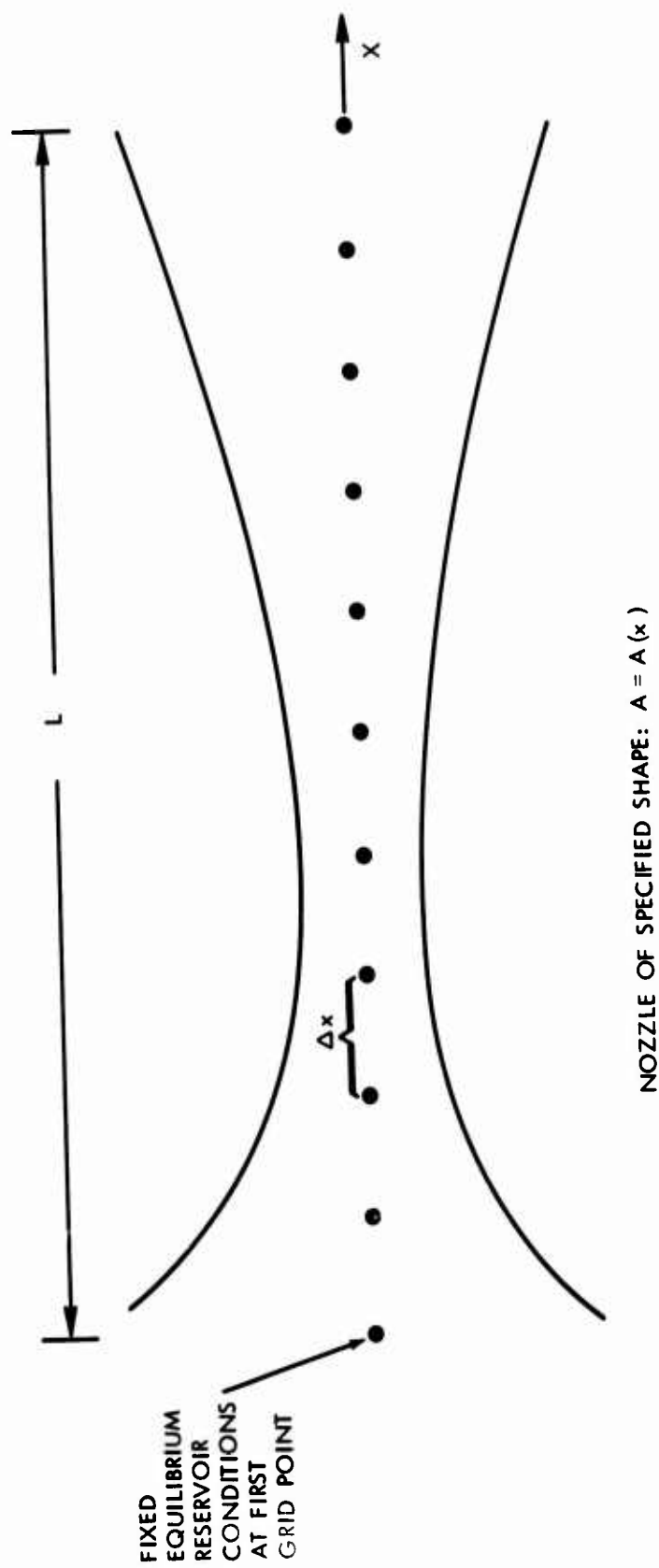


FIG. 1 SKETCH OF THE COORDINATE SYSTEM AND GRID POINTS



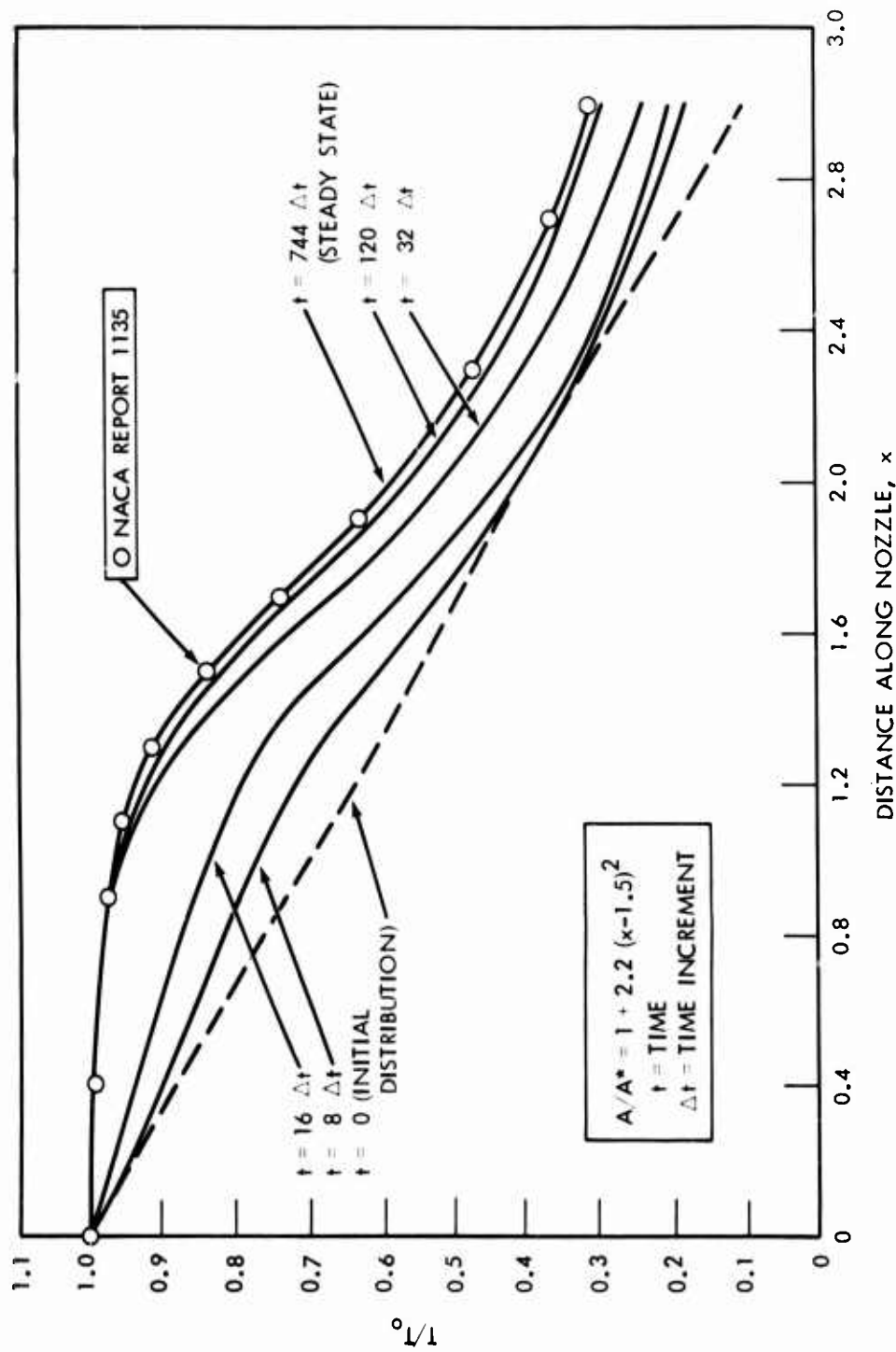


FIG. 2 TRANSIENT AND FINAL STEADY-STATE TEMPERATURE DISTRIBUTIONS FOR A CALORICALLY PERFECT GAS OBTAINED FROM THE PRESENT TIME-DEPENDENT ANALYSIS;  $\gamma = 1.4$

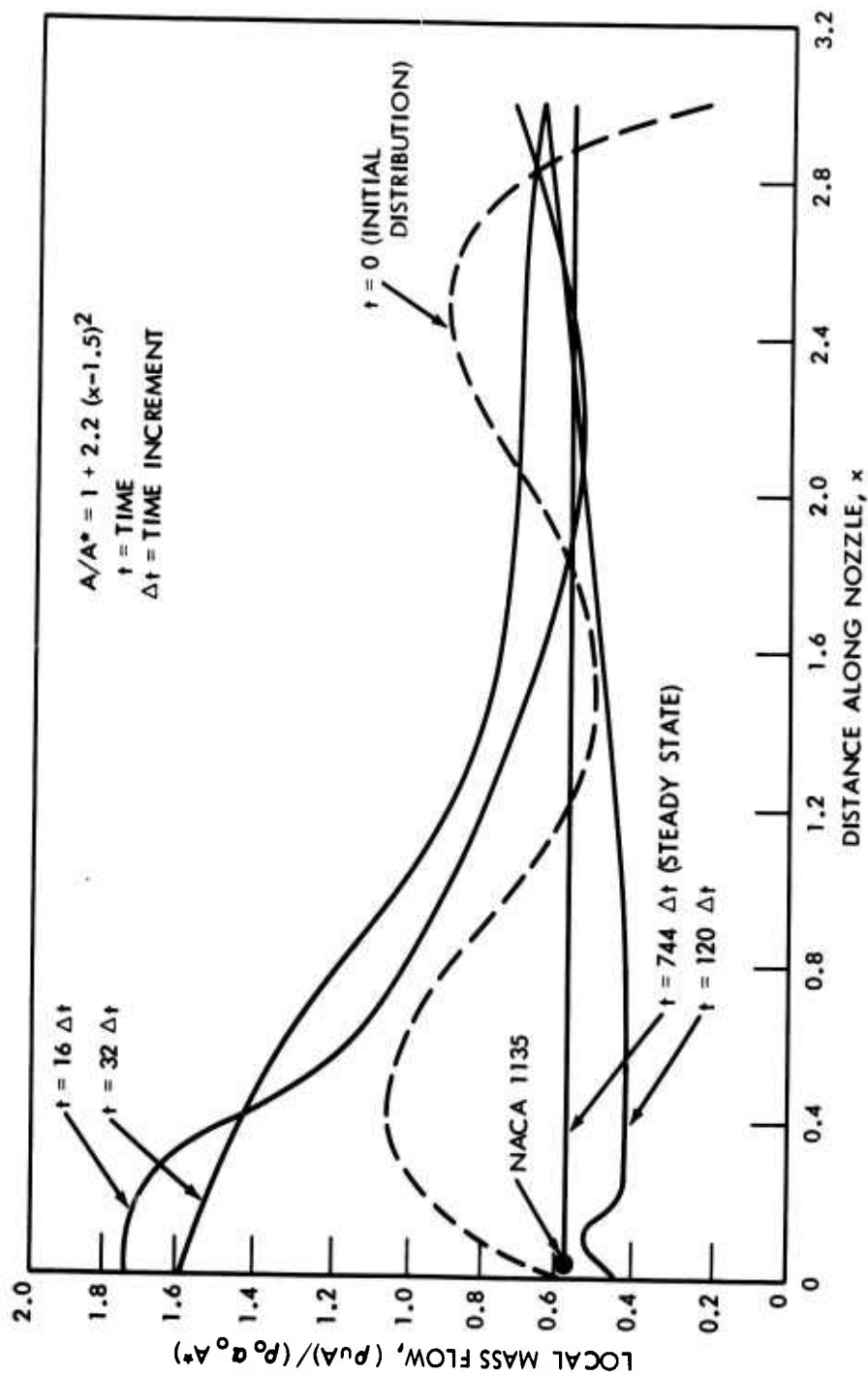


FIG. 3 TRANSIENT AND FINAL STEADY-STATE MASS-FLOW DISTRIBUTIONS FOR A CALORICALLY PERFECT GAS OBTAINED FROM THE PRESENT TIME-DEPENDENT ANALYSIS;  $\gamma = 1.4$

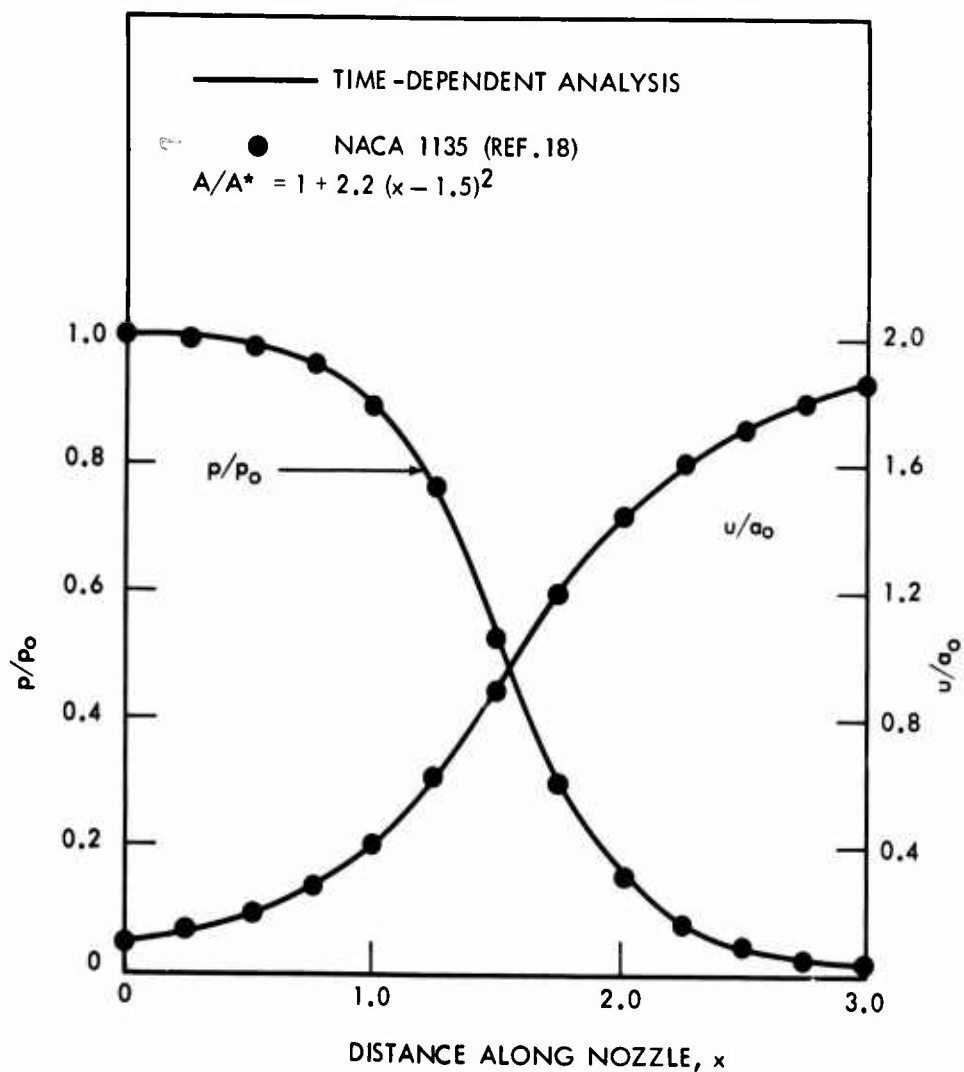


FIG. 4 STEADY-STATE PRESSURE AND VELOCITY DISTRIBUTIONS FOR A CALORICALLY PERFECT GAS; COMPARISONS OF THE PRESENT TIME-DEPENDENT ANALYSIS WITH RESULTS OBTAINED FROM REFERENCE 18.

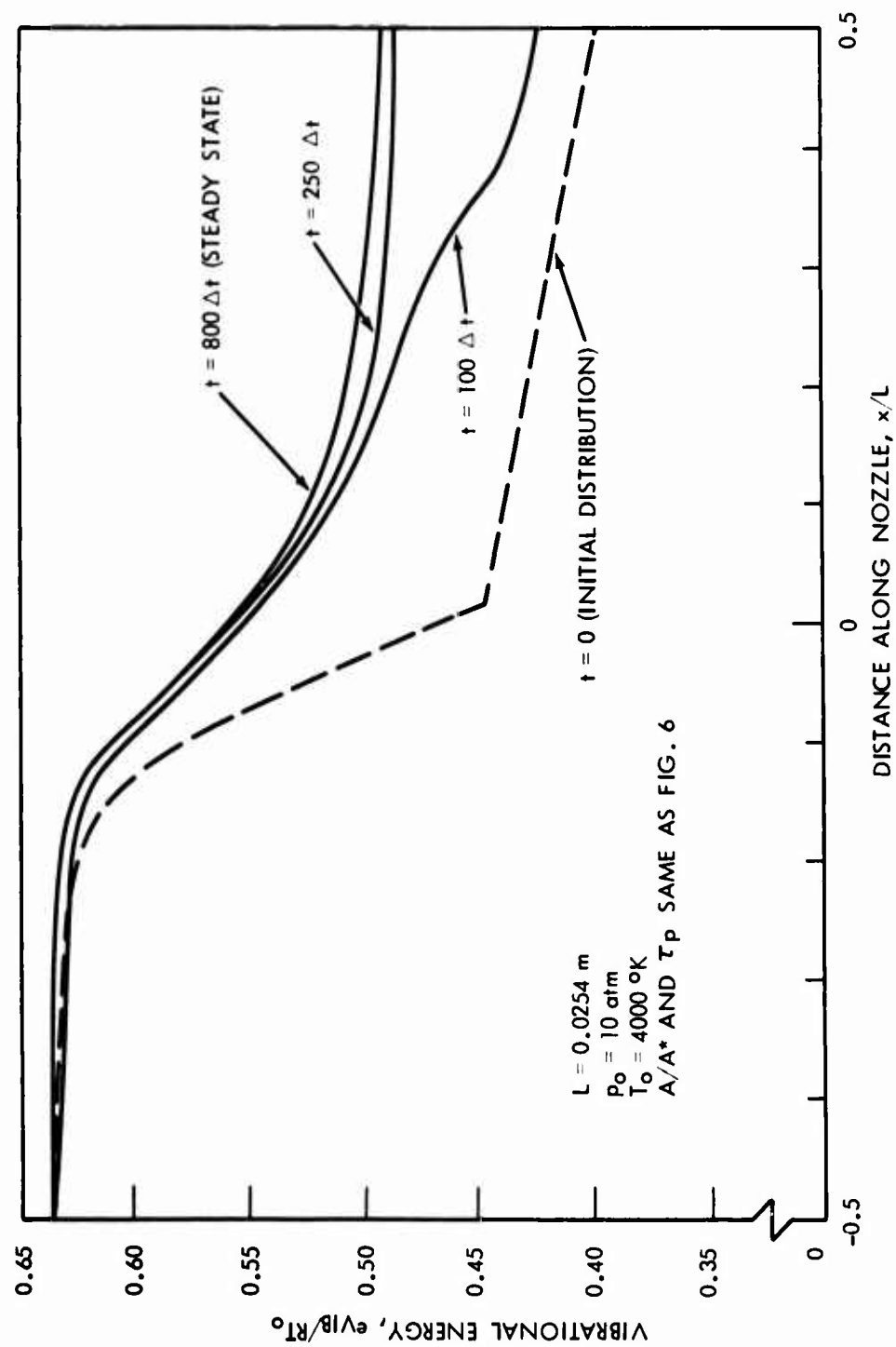


FIG. 5 TRANSIENT AND FINAL STEADY-STATE  $e_{vib}$  DISTRIBUTIONS FOR THE NONEQUILIBRIUM EXPANSION OF  $N_2$  OBTAINED FROM THE PRESENT TIME-DEPENDENT ANALYSIS

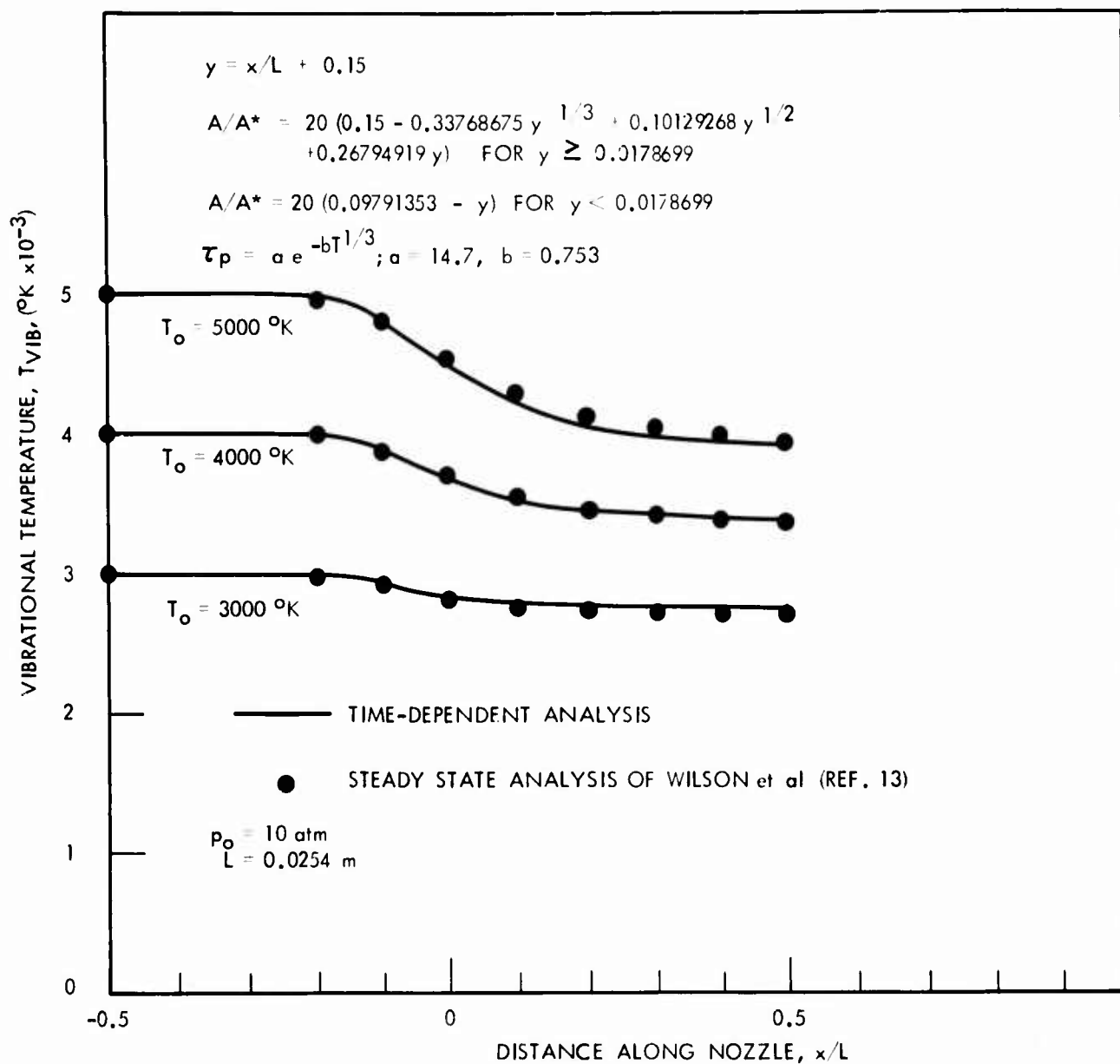


FIG. 6 STEADY-STATE  $T_{VIB}$  DISTRIBUTIONS FOR THE NONEQUILIBRIUM EXPANSION OF  $\text{N}_2$ ; COMPARISON OF THE PRESENT TIME-DEPENDENT ANALYSIS WITH THE STEADY-FLOW ANALYSIS OF REFERENCE 13.

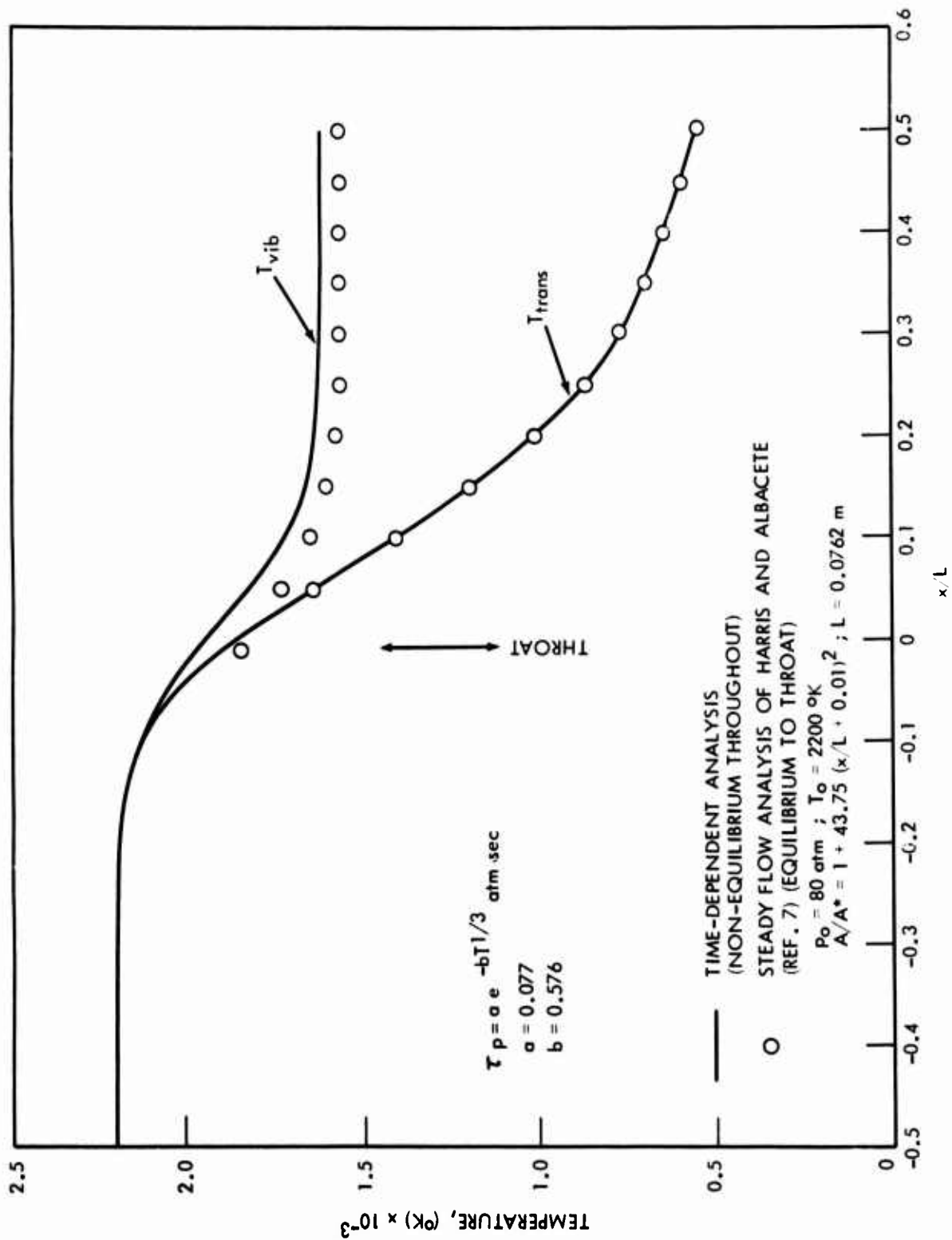


FIG. 7 STEADY-STATE  $T_{vib}$  AND  $T_{trans}$  DISTRIBUTIONS FOR THE NONEQUILIBRIUM EXPANSION OF  $N_2$ ; COMPARISON OF THE PRESENT TIME-DEPENDENT ANALYSIS WITH THE STEADY-FLOW ANALYSIS OF REFERENCE 7.

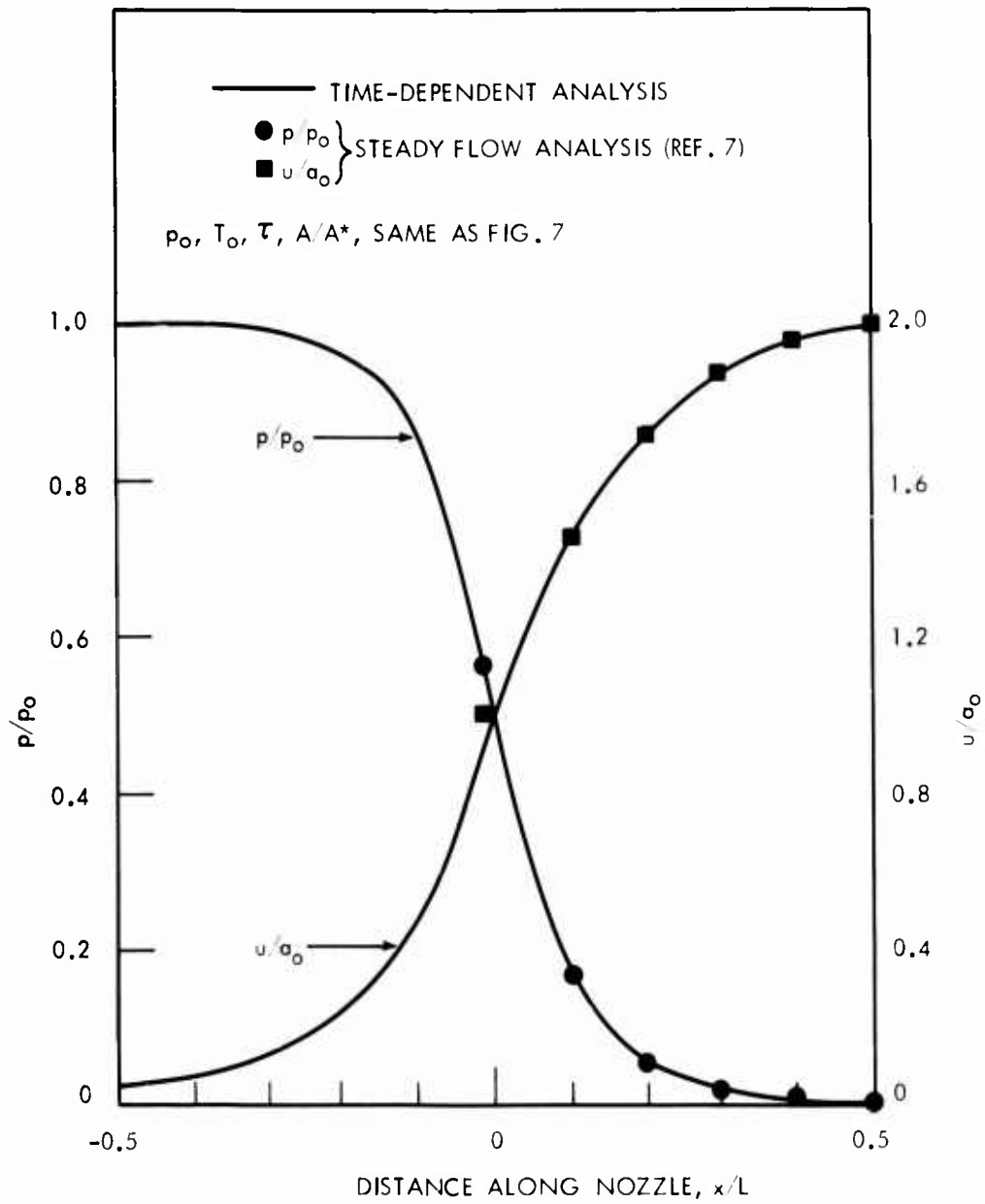


FIG. 8 STEADY-STATE PRESSURE AND VELOCITY DISTRIBUTIONS FOR THE NONEQUILIBRIUM EXPANSION OF  $N_2$ ; COMPARISON OF THE PRESENT TIME-DEPENDENT ANALYSIS WITH THE STEADY-FLOW ANALYSIS OF REFERENCE 7.

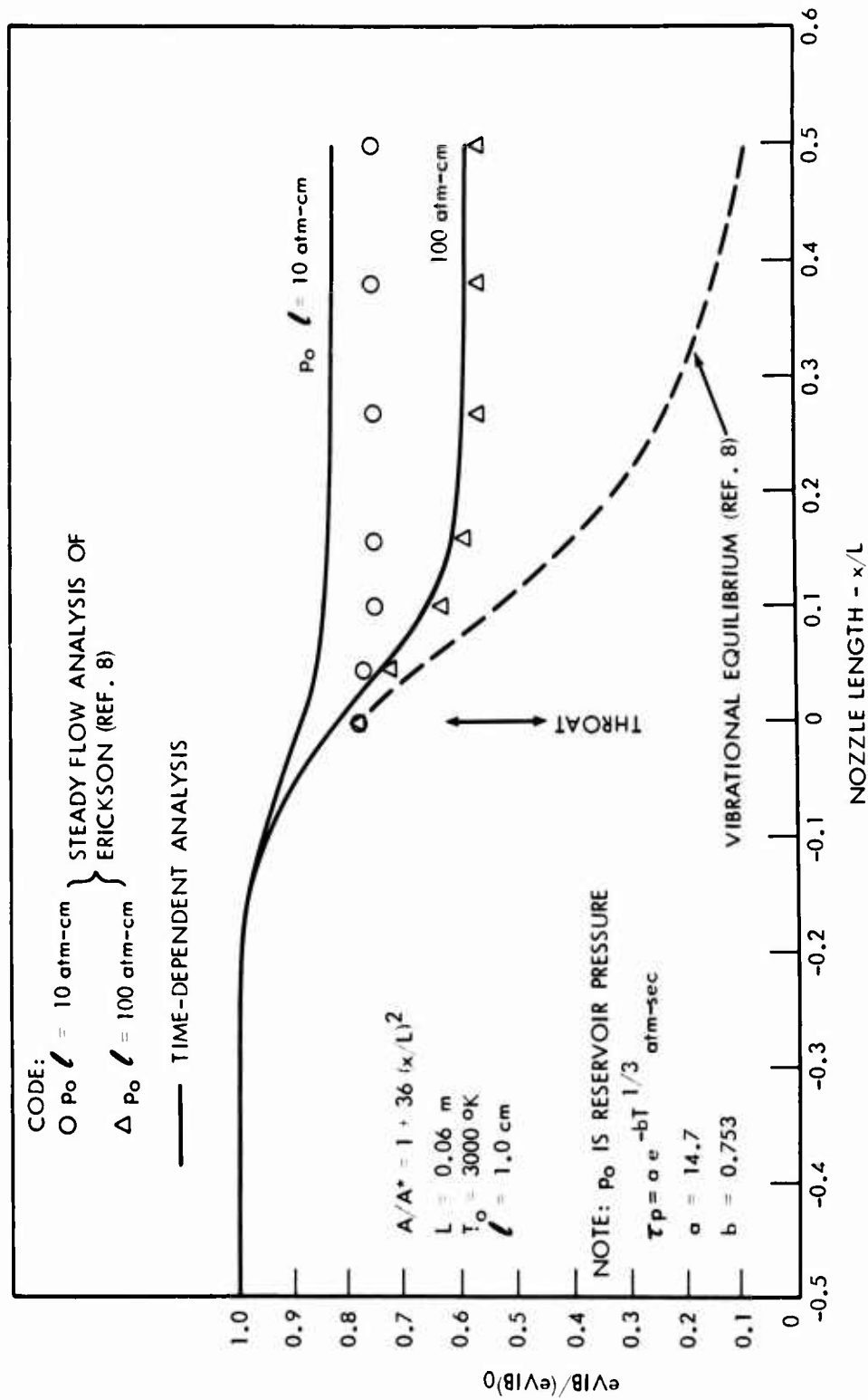


FIG. 9 STEADY-STATE  $e_{vib}$  DISTRIBUTIONS FOR THE NONEQUILIBRIUM EXPANSION OF  $N_2$ ; COMPARISON OF THE PRESENT TIME-DEPENDENT ANALYSIS WITH THE STEADY-FLOW ANALYSIS OF REFERENCE 8.



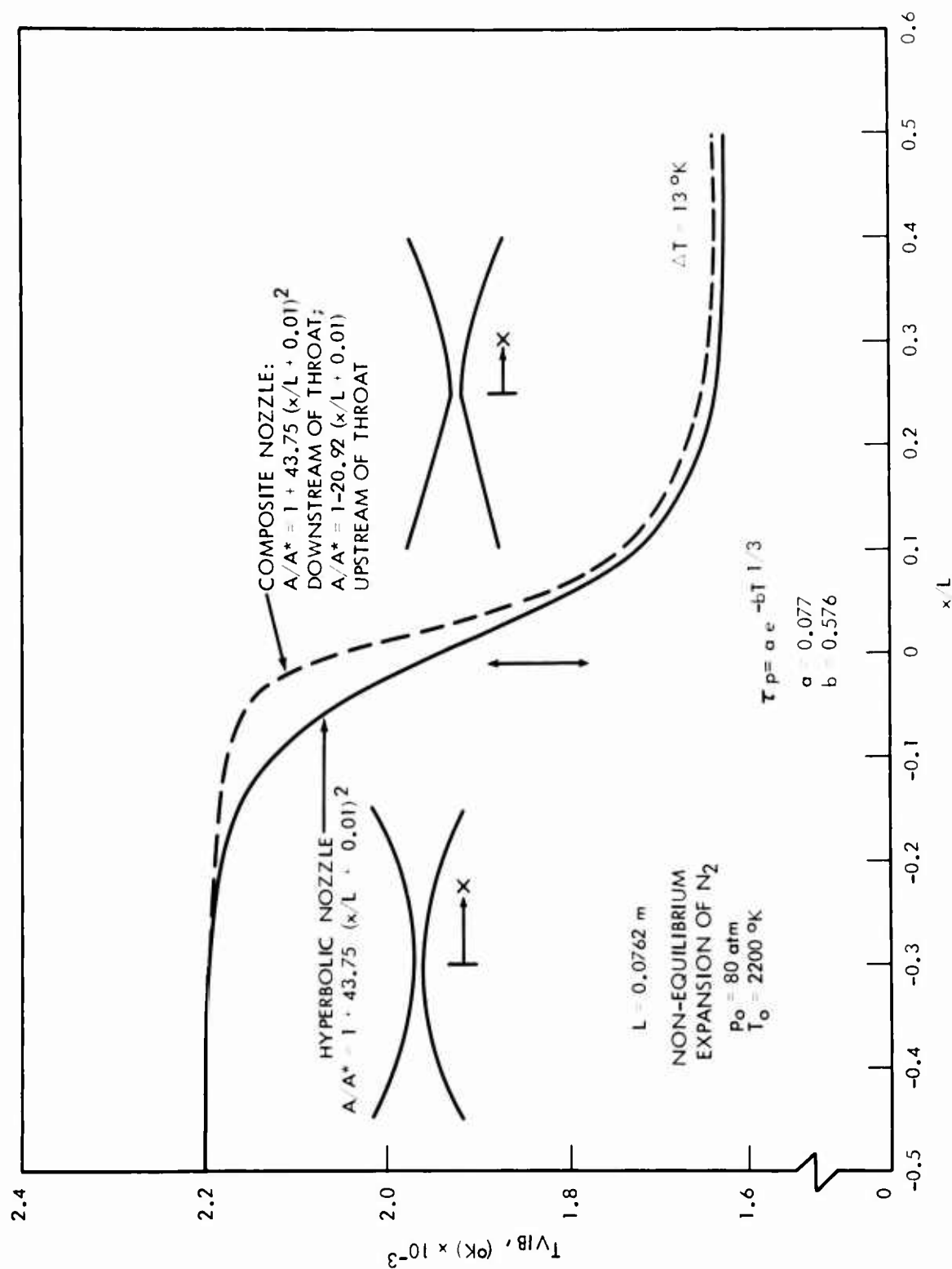


FIG. 10 COMPARISON OF  $T_{vib}$  DISTRIBUTIONS FOR TWO NOZZLES WITH DIFFERENT SUBSONIC SECTIONS BUT IDENTICAL SUPERSONIC SECTIONS;  $p_0 = 80 \text{ atm}$ , NONEQUILIBRIUM EXPANSION OF  $N_2$

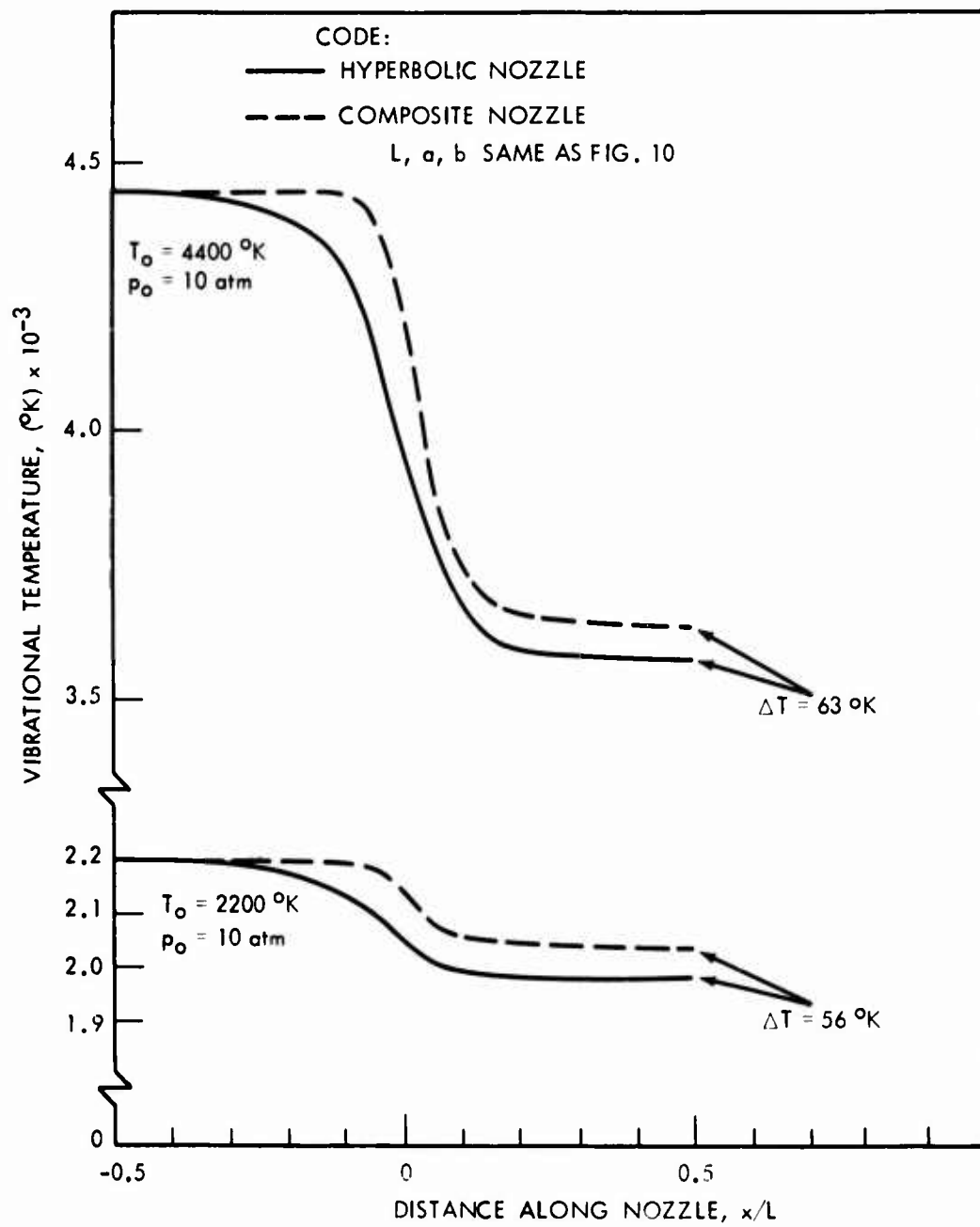


FIG. 11 COMPARISON OF  $T_{vib}$  DISTRIBUTIONS FOR TWO NOZZLES WITH DIFFERENT SUBSONIC SECTIONS BUT IDENTICAL SUPERSONIC SECTIONS;  $p_o = 10\text{ atm}$ , NONEQUILIBRIUM EXPANSION OF  $\text{N}_2$ .

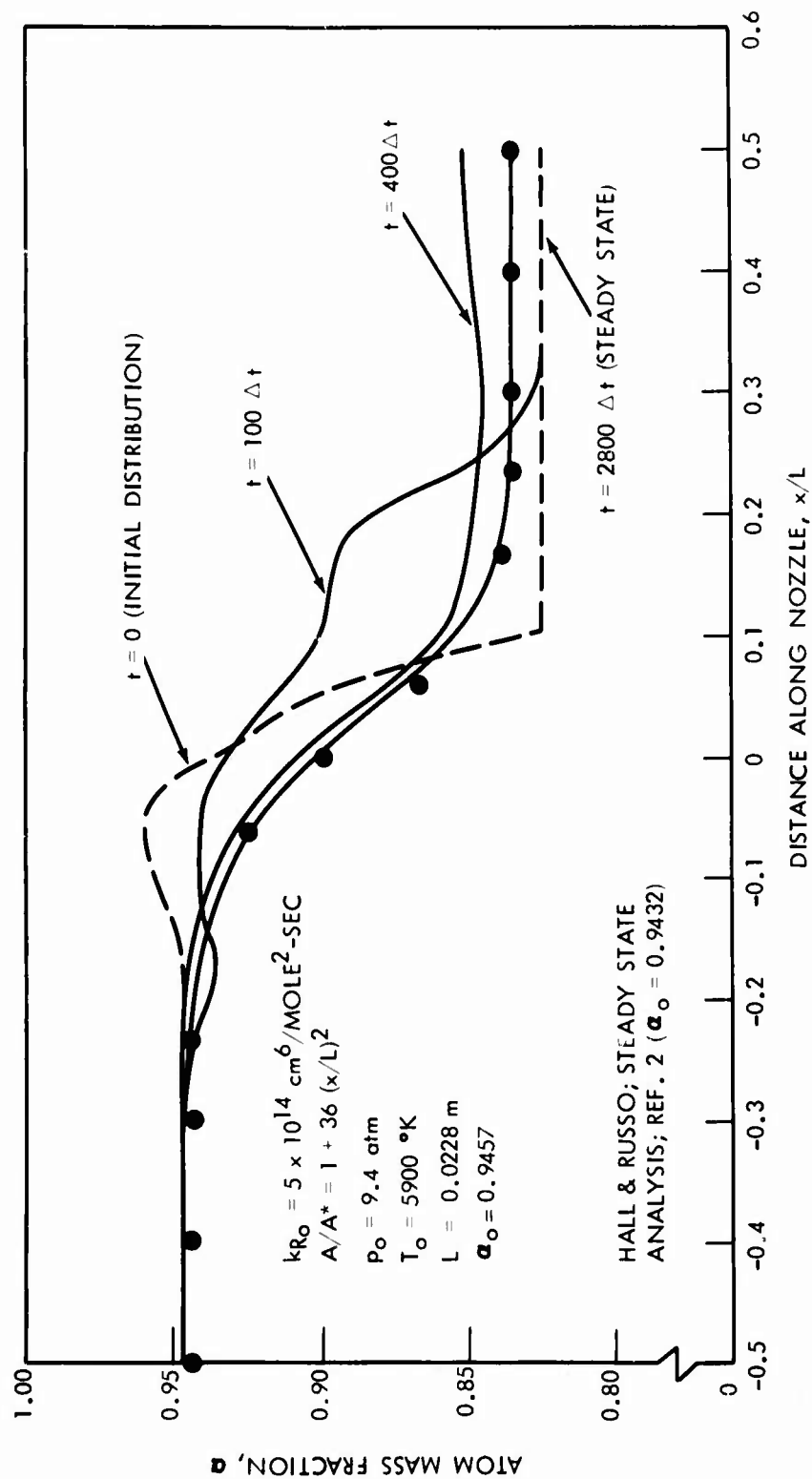


FIG. 12 TRANSIENT AND FINAL STEADY-STATE ATOM MASS FRACTION DISTRIBUTIONS FOR THE NONEQUILIBRIUM EXPANSION OF DISSOCIATING OXYGEN OBTAINED FROM THE PRESENT TIME-DEPENDENT METHOD; THE STEADY-STATE DISTRIBUTION IS COMPARED WITH THE STEADY-FLOW ANALYSIS OF REFERENCE 2.

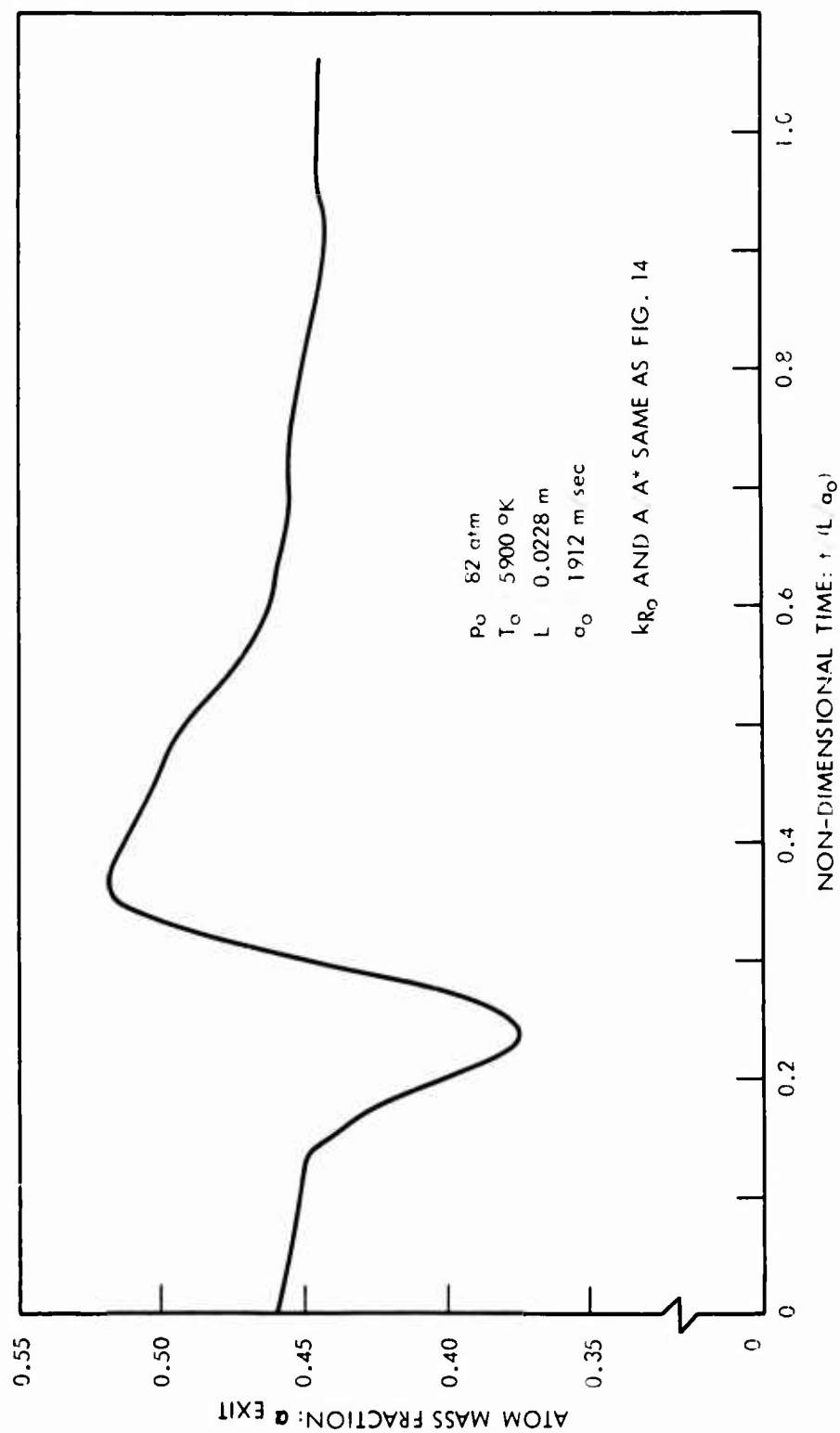


FIG. 13 VARIATION OF ATOMIC MASS FRACTION AT THE NOZZLE EXIT AS A FUNCTION OF TIME.

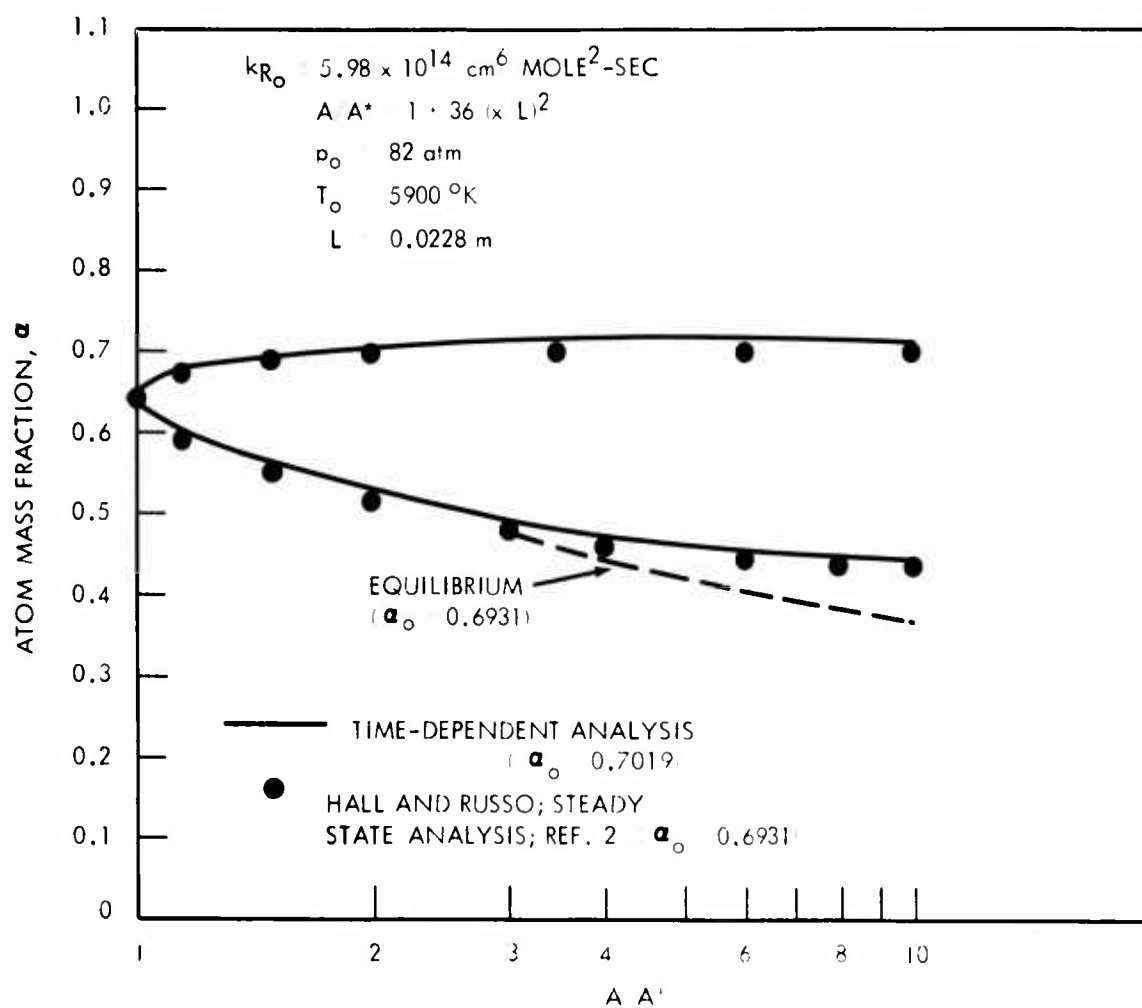


FIG. 14 STEADY-STATE ATOM MASS FRACTION DISTRIBUTION FOR  
 THE NONEQUILIBRIUM EXPANSION OF DISSOCIATING  
 OXYGEN; COMPARISON OF THE PRESENT TIME-DEPENDENT  
 ANALYSIS WITH THE STEADY-FLOW ANALYSIS OF REF. 2

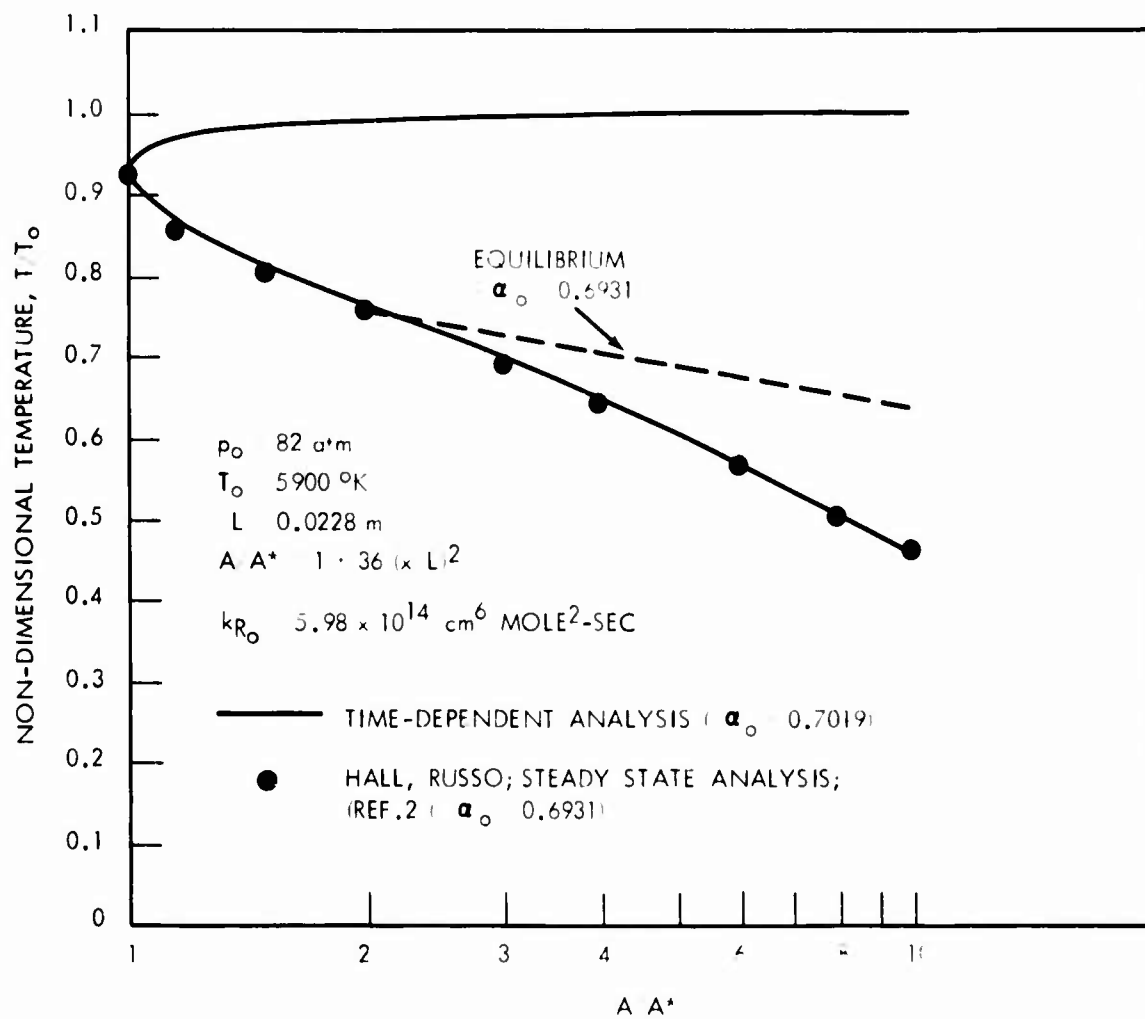


FIG. 15 STEADY-STATE TEMPERATURE DISTRIBUTION FOR THE NON-EQUILIBRIUM EXPANSION OF DISSOCIATING OXYGEN; COMPARISON OF THE PRESENT TIME-DEPENDENT ANALYSIS WITH THE STEADY-FLOW ANALYSIS OF REF. 2

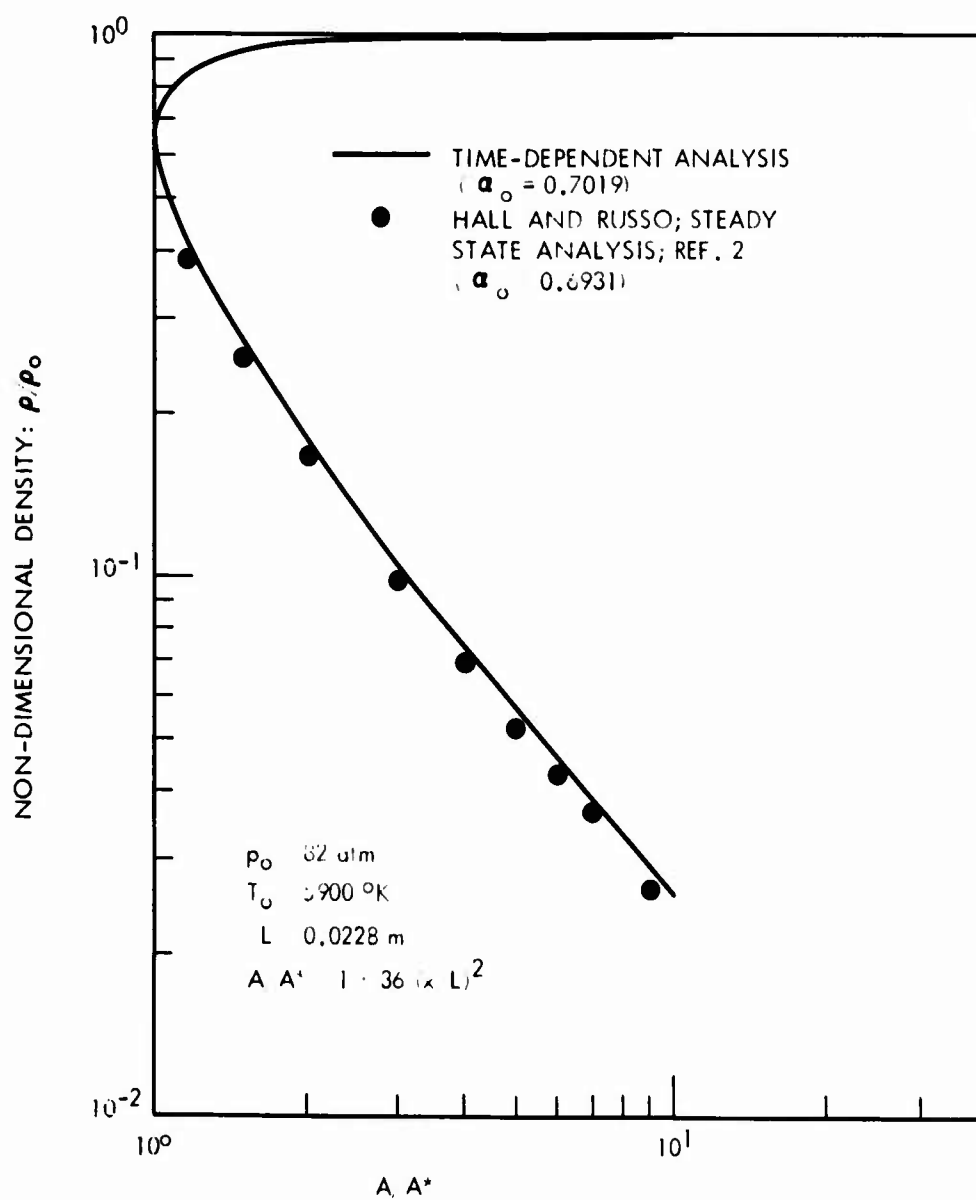


FIG. 16 STEADY-STATE DENSITY DISTRIBUTION FOR THE NON-EQUILIBRIUM EXPANSION OF DISSOCIATING OXYGEN; COMPARISON OF THE PRESENT TIME-DEPENDENT ANALYSIS WITH THE STEADY-FLOW ANALYSIS OF REF. 2

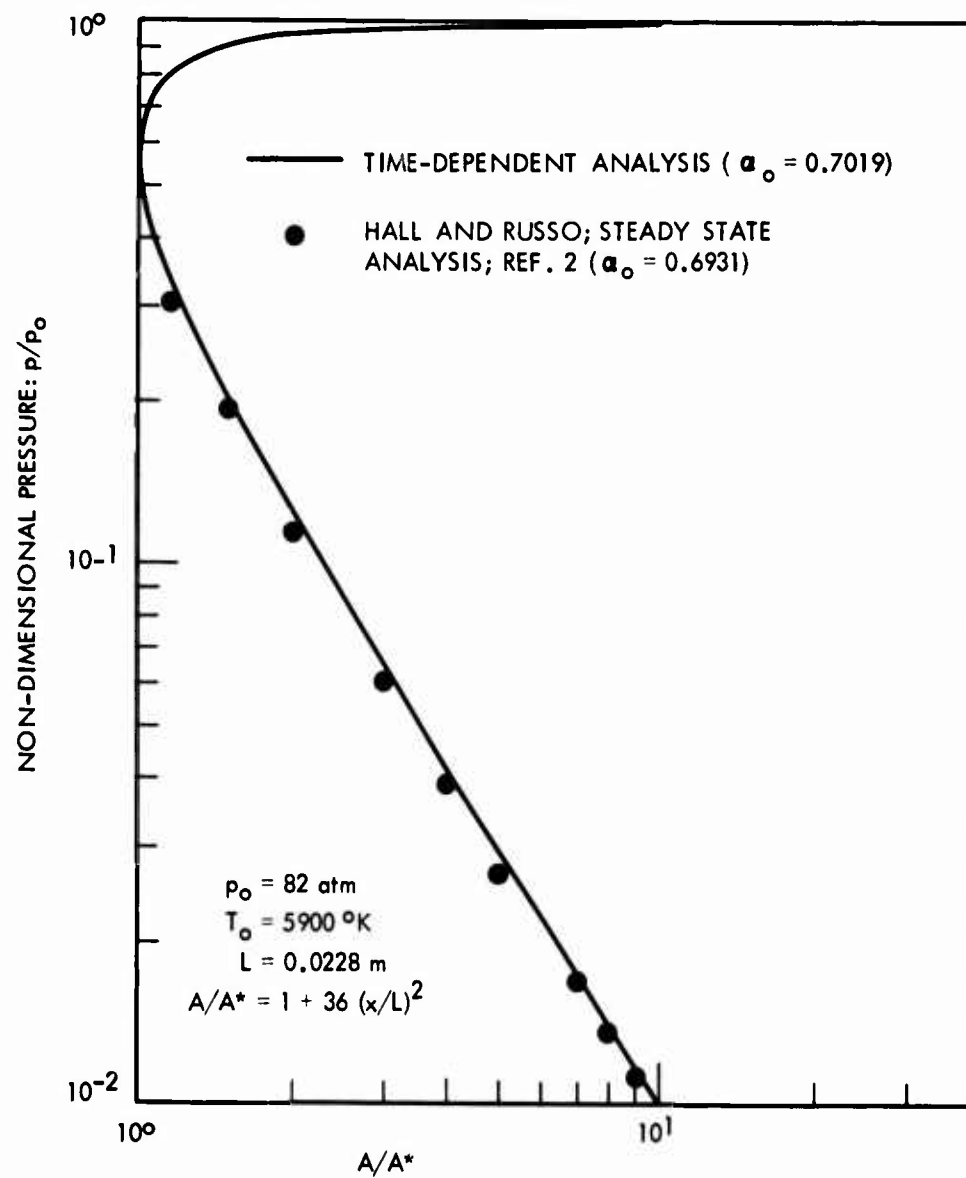


FIG. 17 STEADY-STATE PRESSURE DISTRIBUTION FOR THE NON-EQUILIBRIUM EXPANSION OF DISSOCIATING OXYGEN; COMPARISON OF THE PRESENT TIME-DEPENDENT ANALYSIS WITH THE STEADY FLOW ANALYSIS OF REF. 2



UNCLASSIFIED

Security Classification

DOCUMENT CONTROL DATA - R & D		
<i>(Security classification of title, body of abstract and indexing annotation must be entered when the overall report is classified)</i>		
1. ORIGINATING ACTIVITY (Corporate author) U. S. Naval Ordnance Laboratory White Oak, Silver Spring, Maryland		2a. REPORT SECURITY CLASSIFICATION UNCLASSIFIED
		2b. GROUP
3. REPORT TITLE A Time-Dependent Analysis for Quasi-One-Dimensional Nozzle Flows with Vibrational and Chemical Nonequilibrium		
4. DESCRIPTIVE NOTES (Type of report and inclusive dates) final		
5. AUTHOR(S) (First name, middle initial, last name) John D. Anderson, Jr.		
6. REPORT DATE May 1969	7a. TOTAL NO. OF PAGES 29 plus illus.	7b. NO. OF REFS 25
8a. CONTRACT OR GRANT NO.	9a. ORIGINATOR'S REPORT NUMBER(S) NOLTR 69-52	
b. PROJECT NO. (1) NOL Independent Research c. (2) ONR Fluid Mechanics Branch Attn: M. Cooper d.	9b. OTHER REPORT NO(S) (Any other numbers that may be assigned this report)	
10. DISTRIBUTION STATEMENT This document has been approved for public release and sale, its distribution is unlimited.		
11. SUPPLEMENTARY NOTES		12. SPONSORING MILITARY ACTIVITY
13. ABSTRACT A new technique is presented for the numerical solution of quasi-one-dimensional, vibrational and chemical nonequilibrium nozzle flows including nonequilibrium conditions both upstream and downstream of the throat. This new technique is a time-dependent analysis which entails the explicit finite-difference solution of the quasi-one-dimensional unsteady flow equations in steps of time, starting with assumed initial distributions throughout the nozzle. The steady-state solution is approached at large values of time. A virtue of the present time-dependent analysis is its simplicity, which prevails from its initial physical formulation to the successful receipt of numerical results. Also, the present solution yields the transient as well as the steady-state nonequilibrium nozzle flows. To exemplify the present analysis, results are given for several cases of vibrational and chemical nonequilibrium expansions through nozzles.		

DD FORM 1473 (PAGE 1)

S/N 0101.807.7801

UNCLASSIFIED

Security Classification

UNCLASSIFIED

Security Classification

14 KEY WORDS	LINK A		LINK B		LINK C	
	ROLE	WT	ROLE	WT	ROLE	WT
Nonequilibrium flow Time-dependent analysis Chemical nozzle flows Vibrational nozzle flows Nozzle expansions						

DD FORM 1 NOV 68 1473 (BACK)  
(PAGE 2)

UNCLASSIFIED

Security Classification

END